Travail de fin d'études et stage[BR]- Master's thesis : Design of a District Heating Network and an Energy System in the Industrial Park "Les Hauts-Sarts"[BR]- Stage d'insertion professionnelle

Auteur : Bareel, Pierre-Yves
Promoteur(s) : Dewallef, Pierre
Faculté : Faculté des Sciences appliquées
Diplôme : Master en ingénieur civil électromécanicien, à finalité spécialisée en énergétique
Année académique : 2020-2021
URI/URL : http://hdl.handle.net/2268.2/11600

LIÈGE université
Sciences Appliquées

Graduation thesis with the aim of acquiring a
Master's degree in Electromechanical Engineering

Academic year 2020–2021

Design of a District Heating Network and an Energy System in the Industrial Park "Les Hauts-Sarts"

June 2021

Author: Bareel Pierre-Yves – MSc in Electromechanical Engineering

Supervisors: Dewallef Pierre - Professor at ULiège
Résimont Thibaut – PhD candidate/research engineer at ULiège
Joskin Eva - PhD candidate/research engineer at ULiège

Contents

Acknowledgements

I would like to express my deepest appreciation to my supervisors. To begin, I would like to thank Pr.Dewallef, who accepted to supervise my master thesis and introduced me to the research engineers of the Thermodynamics Laboratory of the University of Liège. Among them, I am extremely grateful to Thibaut Résimont and Eva Joskin, who gave me a lot of valuable advice and helped me overcome some issues.

I would also like to thank Valentin Parys and Valentin Fontaine from ENGIE IMPACT, who presented me their optimisation program `Prosumer` and gave me access to input data files concerning the industrial park of "Les Hauts-Sarts". I also wish to thank Selmane Dakir, who provided me with useful articles.

Finally, computational resources have been provided by the Consortium des Équipements de Calcul Intensif (CÉCI), funded by the Fonds de la Recherche Scientifique de Belgique (F.R.S.-FNRS) under Grant No.2.5020.11 and by the Walloon Region. Special thanks to David Colignon and Thomas Keutgen for initiating me to the use of supercomputers from the CÉCI platform.

Abstract

In today's society, attitudes are increasingly evolving towards environmentally responsible consumption. This concerns all kinds of everyday goods, but also energy as the number of micro-grids and local energy communities is in constant expansion. These systems produce their heat and electricity on-site and promote the use of renewable energies. However, such energy systems are in general costly and require an optimal layout in order to guarantee power security of supply while not investing unnecessary huge amounts of money.

This work aims at providing a tool capable of designing the best configuration and operation strategy of a smart energy system, comprised of a district heating network and renewable energies. For each outline, the overall costs and the carbon footprint are provided. This could greatly help decision-makers that have to consider several schemes at the initial phases of a project. Moreover, having a linear program, the tool can easily be transposed from a case study to another while keeping its robustness.

Three different simulations have been investigated in order to demonstrate the flexibility of the model. The envisaged scenarios enable to study the effect of supply and return temperatures on the optimal design of the heating network. In each case, three different restrictions on CO_2 emissions have also been considered. Doing so, the goal is to build Pareto curves, which represent the overall costs in function of the quantity of CO_2 produced. These kinds of curves help to visualise the compromises between conflicting objectives and can be helpful when designing future energy systems.

On the one hand, the results showed that low-temperature district heating networks were best-suited if the main goal is to reduce greenhouse gas emissions. On the other hand, if the attention is rather put on reducing costs, higher supply temperatures at 90°C better fit this motivation. In any case, mid supply temperatures of 70°C were found to be less beneficial.

Nomenclature

4GDH	4^{th} generation district heating
chp	Combined heat and power
COP	Coefficient of performance
DHN	District heating network
EU	European Union
HP	Heat pump
MILP	Mixed-integer linear program
NDC	National determined contribution
NG	Natural gas
PNEC	Plan national énergie-climat
PV	Photovoltaic

Chapter 1

Introduction

Climate change is nowadays a worldwide concern and countries attempt to implement strategies to reduce their greenhouse gas emissions. The best known international plan is probably the Paris Agreement on climate change that was adopted during the COP 21 in 2015. It was approved by 196 parties including Belgium. The major objective of the agreement is to limit the effects of climatic change by containing the global temperature rise significantly below 2°C. The desired temperature rise is 1.5°C compared to the pre-industrial temperature levels [1]. In Europe, The EU has established the European Green Deal, which is an action plan in order for the European Union countries to be climate-neutral in 2050 [2].

In 2020, the participating countries had to present their National Determined Contributions. NDCs are strategic plans, in which countries have to communicate their measures in order to reduce their greenhouse gas emissions. In this context, Belgium handed over the *"Plan national énergie-climat"*, that lists the fixed goals for the period 2021-2030 [3]. However, at the end of the year 2020, the European Commission evaluated Belgium's PNEC and concluded that a lot of points were still to be improved. One of them concerned renewable energies as their proportion in Belgium's total energy mix was considered too low. Though, a rapid expansion happened between the years 2019 and 2020. FIGURE 1.1 shows a percentage of renewable energies (without biogas) of 18.6%, against 14% in 2019 [4]. Other subjects that didn't satisfy the European Commission were the energy efficiencies in buildings, the security of supply and the internal energy market. The latter lacked of measures and objectives concerning the flexibility when using renewable energies, storage systems and interconnected smart grids [5].

Regarding these weaknesses in the Belgian plan to accomplish the national climate goals, some progresses have to be done in the conception and management of energy systems. Against this background, the purpose of this graduation thesis is to present a model that optimises a future sustainable energy system, which takes heat and electricity demands into account. In particular, this model aims at finding the economically optimal design and operational strategy of a district heating network.

In the past, several studies highlighted the potential of district heating networks in Europe, such as the two heat road maps written by CONNOLLY *et al.* [6] [7]. The first article studied different scenarios in which the percentage of space heating provided by DHN is increased in 2030 and 2050. In all scenarios, the results demonstrated that district heating networks increased the efficiency of the energy system and reduced the carbon emissions as well as the overall costs. The second one analysed the local heat demands and heat supplies across the EU27 countries

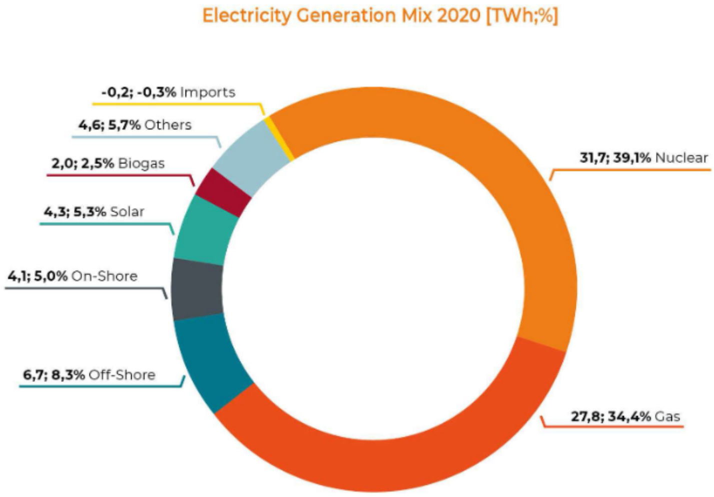

Figure 1.1: Belgium's energetic mix in 2020 [4].

in order to find new district heating potential locations and determine their impact using models. The result was that district heating networks are able to reach the emission targets of 2050, while remaining less costly than alternative solutions focusing on heat savings. Several northern countries have already largely adopted this heating method. For example, more than 60% of Danish households are connected to district heating networks. This ratio increases to 95% in major cities [8].

After having mentioned the potential of district heating systems in the future, it is important to describe their historical background in order to clarify which particular network has been used for this model. Until now, there has been 3 generations of DHN and a 4$^{\text{th}}$ one is being given more and more importance as it responds to the modern requirements. A comprehensive review of the four generations has been written by LUND *et al.* [9].

The first generation appeared at the end of the 19$^{\text{th}}$ century and was used until 1930. Most of these networks were replaced by newer generations but some are still in operation today in certain areas of New York and Paris. At that time, the motivation to install such a network was to reduce the risk of boiler explosions and to raise comfort. The heat carrier was steam at a temperature range of 200-300°C and it was distributed in concrete ducts [10]. However, the disadvantages of the first generation are that some severe accidents happened in the past and that heat losses are important when transporting high temperature steam, leading to a decrease in efficiency.

The second generation of district heating lasted until the 1970s and worked with pressurized hot water at supply temperatures above 100°C. The primary reason for operating this way was to increase the efficiency of the DHN as there would be less heat losses. Another reason was to enhance the expansion of chp utilisation. Lastly, this generation also marked the appearance of tube-and-shell heat exchangers.

The third generation has been largely used from the 1980s until now. The heat carrier is still pressurised water but at a temperature lower than 100°C. This is still a choice to increase the energy efficiency, which was a motivation at that time following the two oil crises. A significant improvement has been made in the materials used for the different components. For instance, heat exchangers are made in stainless steel and pipes are prefabricated. This reduced the manpower needed at the construction sites.

The fourth generation of district heating networks has a different source of motivation compared to previous versions. Indeed, the objective of this modern thermal grid is purely environmental and oriented towards the 2050 challenges introduced in the beginning of this thesis. This is not equivalent to the past economic ambitions, which focused on the reduction in fuel consumption and costs of materials for network components. In the purpose of continuously increasing the efficiency, the 4GDH follows the trend by lowering the supply temperatures as it operates in ranges between 70°C (supply) and 30°C (return). These low distribution temperatures will once more decrease the heat losses in the pipes. Concerning the elements of the DHN, plate heat exchangers will probably be used as well as pre-insulated flexible pipes.

This new generation also permits heat production from centralised and decentralised sources. This means that consumers are able, if it is economically and environmentally beneficial, to feed the heating network with thermal energy from their individual heat source. These types of end-users are sometimes called *prosumers*, which is a term already employed in smart electricity grids. Furthermore, it is important to note that 4GDH is a notion that not only focuses on heat distribution. In fact, the development of 4GDH also involves the renovation of buildings into more energy efficient ones. This will lower the heat energy demands and is considered in the *renovation wave strategy* of the European Green Deal [11].

Then, another major uniqueness of the fourth generation is that it should be integrated in a large-scale smart energy system. This way, some interesting interactions between heat and electricity sectors may appear. For example, the electricity produced by renewable energies could now be able to operate heat pumps. Therefore, 4GDH is often referred to as a *smart thermal grid* and has to be combined with a *smart electricity grid*[1] to maximize the synergies as much as possible. Besides enhancing the integration of renewable sources, the conception of complete smart energy systems adds some flexibility to the national electrical grid. HENNESSY *et al.* [12] highlighted the future increase of variability in electricity prices due to the expansion of stochastic energy sources such as photovoltaics and wind turbines. The article also featured the contribution of these new *smart thermal grids* in balancing the electrical grid. This can be done by varying the power output of chp plants or by controlling the electric consumption of heat pumps. The latter could be increased and produce surplus heat, which could be stored in the different storage tanks located in the district.

The illustration in FIGURE 1.2 reviews the evolution of district heating with time. As mentioned, the efficiency curve increases with decreasing distribution temperatures. It is also observable that for smart thermal grids, at the right of the image, a lot of renewable sources are added and the electricity sector is interacting with the heating sector. When designing future district heating infrastructures, the latest generation of DHN has to be considered for the environmental reasons explained in

[1] It could also be combined with *smart gas grids* but this option is not taken into account in this model.

the beginning of the introduction.

To do so, the present model will optimize the amount of installed heat and electricity productions as well as their operation throughout the year. The design of the optimal mix can go from 100% centralised to 100% decentralised. This means that solutions can vary from a large central plant to several decentralised heat sources. It will depend on the inputs of the model and will be discussed later.

The case study on which the model has been applied is an industrial park called "Les Hauts-Sarts" in Liège, Belgium. The optimisation will decide which technologies to install in the area in order to minimize the costs over a project duration of 20 years. Some parameters and inputs will be studied to see the influence they can have on the optimal mix. In particular, three different supply temperature levels will be investigated in chapter 4. Moreover, depending on the CO_2 limitations, the configuration of the DHN may have a certain topology or another. At the end, it will also be possible to draw a Pareto curve showing the total costs as a function of the total CO_2 emissions. This curve is interesting as it will put a number on the investment and operation costs needed to fulfill the environmental challenges in that area.

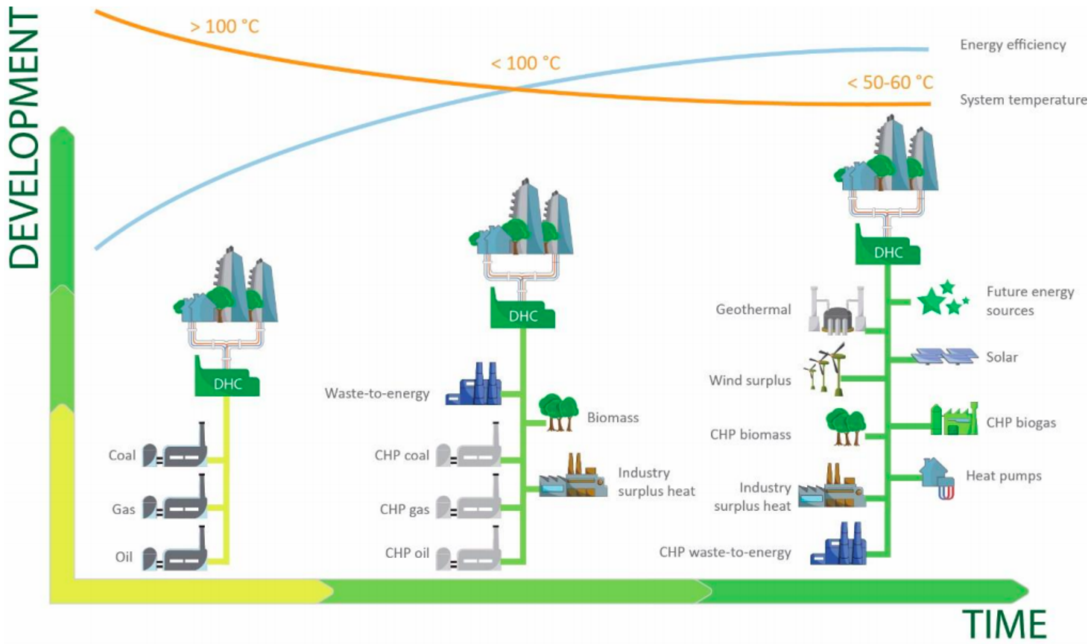

Figure 1.2: Evolution of district heating networks through the years [13].

1.1 Literature review

The benefits from district heating networks are only visible when the system is well-designed and well-operated. Hence, a large number of researches have been undertaken to find the optimal energetic mix. Most of these studies make use of mixed-integer programming to compute their optimisation models. The specificity of such programs is that they contain both binary and continuous variables. On the one hand, binary variables are generally responsible for choosing or not to install a technology or a pipe connection at a specific location. On the other hand, continuous variables are primarily assigned to the amount of capacity installed or the power produced at a certain time by a technology. The combination of these two variables makes this programming type perfectly fitted to find adequate layouts on an existing site.

Nowadays, several variants of mixed-integer programs exist and each have their own characteristics. The most important distinction is whether the equations are linear (MILP) or non-linear (MINLP). First, a brief review of MINLP articles will be reported. This will highlight the situations in which they are efficient as well as their pros and cons.

MERTZ *et al.* [14] proposed a tool that optimizes the configuration of the network layout and the production technologies. Simultaneously, it optimizes the size of each power source. The authors' wish was to precisely describe the operation of the energy productions so that the installed capacities were the most optimal possible. To do so, the design variables corresponding to the sizing aspect are the temperatures, the velocity and the diameter of the pipes. The tool is thus very precise in terms of network operation, e.g. it is able to compute thermal losses and pressure drops. The counterpart is that it has nonlinearities in its energy balance equations. It increases the complexity of the model such that the time needed to resolve simple cases is huge. Consequently, the optimization was made for only one period (single period MINLP) and storage systems could not be taken into account.

Other MINLP programs decided to focus on optimizing of the control and scheduling of a district heating system. This is the case of the article written by DENG *et al.* [15], which proposes a day-ahead optimal scheduling strategy based on actual operational data from an energy station in Tianjin. The optimization is based on the minimization of daily operational costs. The energy station is composed of a multitude of technologies to meet the heat and cooling demand in the area. Results showed that the cost-saving ratio could reach values between 24.3% and 63.9% depending on the load ratio.

KRUG *et al.* [16] also oriented their research towards a MINLP for the dynamic time-dependent control of heating networks. In this case, the constraints are subject to non-linear partial differential equations representing the physics of water and heat flows. The equations are then discretized in space and time to make the problem tractable. The applicability of the technique was proved on numerical test cases.

A common tendency related to mixed-integer non-linear programs is the time-consuming computation needed to find a solution to the optimization problems. This is a first limitation to non-linear programs. It was observed in MERTZ *et al.* [14], where only a single period was handled, and in DENG *et al.* [15], where the problem is solved for the coming 24h. A second limitation is inherent to the way MINLPs are managed by the solvers. In fact, when a non-linear program is solved, a local solution is identified but nothing guarantees that it is a global solution, i.e. the best feasible. Both limitations are due to higher complexity and are the price to pay for better precision on non-linear behaviours.

As a reminder, the objective of the given model is to get the optimal design of smart energy systems in an industrial park. This usually involves dealing with several periods over the year, e.g. including storage and taking different load profiles into account. The model should also be easily scalable so that it can be useful for any case study. Hence, MINLP is not so well-suited for this kind of problem and mixed-integer linear programs (MILP) will be used instead. This outcome was quite expected as most of the articles in the literature about optimal sizing of district heating networks are computed with MILP and only a few with MINLP. Non-linear programming will thus frequently be used for short-term control in existing district networks and it will focus on dynamic modeling by taking physical variables into account (temperature, mass flow rates, etc.).

Now that the choice of a MILP has been justified, the following paragraphs will review the studies available in the literature for linear programs of the same topic. Alongside the evolution of district heating networks, the content found in literature followed a similar path. For instance, older papers written during the period 2000-2010 did essentially focus on the 3rd district heating generation, while later papers referred to the 4th generation. First, a revision of older studies will be done and it will be pursued by a second one related to newer papers.

SODERMAN *et al.* [17] presented an approach to optimize the outline and the design/operation of distributed energy systems (DER), including a potential network for district heating. The test case included three alternatives for energy sources : chp or boilers for heat demands and wind turbines for electricity demands. Heat storage was also taken into account. Only eight values were used to create a yearly heat load profile for all the consumers. The MILP objective minimizes the total costs, which are formed by the overall running costs and the annualised investment costs of the equipment.

CASISI *et al.* [18] based their research on a real city center, in the municipality of Pordenone (Italy). The model looks for an optimal layout and operation of a DER. The program only considers chp technologies to meet both heat and power needs. If the decentralised option is chosen for a building, a micro-turbine is installed at that node. Otherwise, an internal combustion engine is installed for a centralised option and a district heating network feeds a subgroup of buildings. The MILP objective function minimizes the cost of owning, maintaining and operating the whole system. In this situation, the results demonstrated that it would be profitable for the six buildings of the case study to install a micro-turbine and thus not constructing a district heating. Though, the optimal solution could be affected by the investment cost of the technologies or the economic policies taken into account by the municipality.

WEBER *et al.* [19] developed the tool DESDOP, which aims at providing the best mix of renewable and non-renewable energies in a small city. Any energetic combinations can vary from 100% centralised to 100% decentralised. The locations where decentralised technologies are installed can be connected to the network and use this supplementary energy supply during peak demands. The consumers can, however, not discharge energy back to the network. The variety of technologies was greater in this paper : heat pumps, chp, wind turbines, photovoltaics, solar thermal collectors. The case study included mostly residential but also non-residential buildings, counting for a total of 6500 inhabitants. The conclusion was that the site could not yet be 100% renewable as fossil-fueled electricity production or imports from the grid were still needed to sustain consumption. The best choice according to heat production, was to install heat pumps and chp plants. A very few amounts of PV panels were installed because ten years ago, the investment cost was high (7500£/kWp)[2].

Up to now, the given articles don't really correspond to modern *smart thermal grids*. A first reason is that these works date back to a period before 2010, during which

[2]Today, prices are ten times lower such that values between 720 and 740 €/kW can be found on the market.

this modern approach was not yet investigated. Then, the number of available technologies in the previous studies was quite limited, which is contradictory to new *smart energy systems*, that consider a wide range of renewable and non-renewable technologies. In addition, none of the presented articles did minimize the carbon emissions in their objective functions, which is an important aspect of 4GDH. Finally, the roles of the individuals were fixed, i.e. no heat *prosumers*, limiting the possible synergies on-site. The next articles were written after 2010 and are more related to modern optimization tools for 4^{th} generation district networks.

MEHLERI *et al.* [20] and OMU *et al.* [21] had a similar approach in the implementation of their models. Both articles aim at finding the optimal design of distributed energy systems and at selecting technologies with predefined capacities. The two MILPs minimize the total annualised costs and include a cost for CO_2 emissions based on carbon taxes. None of the papers added heat storage in their studies. One of the scenarios of OMU *et al.* [21] was to observe which degree of decentralisation[3] was the best for the test case. The results demonstrated that it was very dependent on the characteristics of the site. In that specific case, district scale networks were sub-optimal compared to building scale distributed technologies[4]. It is also reported that subsidies play an important role in the technology selection and show once more the dependence on the economic-regulatory context of the area. Regarding MEHLERI *et al.* [20], the model was applied to a fictitious neighbourhood of 20 buildings and the result showed that micro-chp sources and boilers were used in half of the buildings to produce thermal energy for all the district heating network.

BUORO *et al.* [22] declared that purely economic analysis is no more sufficient and that environmental aspects have to be taken into consideration. Hence, the objective function is a linear combination of the total annual costs and the CO_2 emissions associated with the system. The weights can be modified to observe the impact on the optimal solution. The test case concerned an industrial area in Northern Italy. With this climatic condition, only solar fields were envisaged for the central plants, whereas boilers and chp plants were accepted for decentralised locations. The result demonstrated that, among all the scenarios, the solar central plant coupled with heat storage and district heating was the most convenient economically and environmentally.

MORVAJ *et al.* [23] is the most recent paper from this review and proposed a very comprehensive method for *smart thermal grid* optimisation. In this case, the heat and power plants can only be installed in the buildings and no centralised locations are provided. Therefore, the system is called a decentralised district network, in which all the production and consumption comes from the *prosumers* linked together. The carbon emissions are limited by constraints and not conflicting objective functions like carbon taxes. The potential technologies to be selected at buildings include boilers, chp, photovoltaics, solar thermal panels and thermal storage. The test case is constituted of a fictitious neighbourhood made of 12 buildings. The results revealed that, for the same price, 33% of CO_2 savings could be achieved compared to the business-as-usual case[5] when all the technologies were integrated and a district heating network was constructed. Moreover, the more restrictive the limitations on carbon emissions were, the more connections were established in the

[3]Three degrees of decentralisation : building scale, district scale or the two combined.
[4]Biomass chp was essentially used
[5]Natural gas boilers for all the heating consumption.

network.

After reviewing the latest papers related to district energy system optimisation, a few comments have to be discussed. Foremost, a common similarity between [20–23] is that they all consider environmental measures either as a carbon tax in the objective function or as a constraint. When this is added in the objective function, the MILP is said to be multi-objective, in contradiction to single-objective, e.g. the first articles taking only costs into account. Then, the number of technologies that are usable on-site was generally higher than in the older articles. These additions to the scientific research correspond well to the characteristics of *smart thermal grids*, which promote environmental regards and a variety of energy sources.

However, some limitations prevail in the different studies. Indeed, a bunch of representative days were adopted to plan the operations over the whole year. This reduces the computing times at the expense of some precision since only a few heat and power demands are input into the model. Consequently, electricity prices and revenues are often taken constant over the whole period, limiting the synergies and the representation of the operations. Another drawback regarding certain articles is that their studies are based on fictitious test cases. This means that they are not connected to a geographic information system (GIS), which enables to implement a model on real district areas and understand the spatial relationships. Therefore, improvements are still possible concerning the research in energy systems optimisation in order to create a complete and detailed model to help decision-makers in their future choices regarding future environmental challenges.

The MILP presented in this master thesis pursues the work that has been initiated in 2017 by Thibaut Résimont, PhD candidate and research engineer at the Univeristy of Liège. The study proposed a MILP optimisation model for the outline and sizing of district heating networks connected to a GIS. The study focused on the centralised plants and networks needed to meet the heating demands in the city of Herstal. Heating consumption was taken edge per edge because of the huge number of inhabitants (more than 40,000), making it intractable to consider the energy demands node per node (each building). Several modifications have thus been applied to the initial model to integrate electricity consumption and the aspects of *smart thermal grids* in the context of an industrial park. TABLE 1.1 resumes the properties of each article from this literature review and highlights the modifications added in this thesis.

This summary table was inspired by a similar one made by Thibaut Résimont in [24]. One of the purposes of this table is to observe the properties added to the previous model of the University of Liège. These modifications are represented with green checkmarks in the table. The term 4GDH stems for fourth generation of district heating networks. This means that articles having a positive mark in that column take CO_2 savings into account as well as renewable power and heat resources and the possibility to be a prosumer in both heat and electricity sector. Then, "100% C-D" tells that the optimisation program is able to find any optimal mix between 100% centralised and 100% decentralised. A last term to be explained is EoS, which considers if the article takes the economy of scale in the costs of the technologies. Another difference between the initial model of ULiège and the one presented in this thesis is the objective function. In fact, on the one hand, the aim is to maximize the net cash flow, taking revenues from heat sales into account. On the other hand, the objective function minimizes the total annualised costs (without revenues) and

Authors	Objective function	Linear	Multi-period	GIS	4GDH	100%C-D	EoS
Mertz	min C_{tot}	✗	✗	✗	✗	✓	✗
Deng	min OPEX	✗	✓	✓	✗	✗	✗
Krug	min OPEX	✗	✓	✓	✗	✗	✗
Soderman	min C_{tot}	✓	✓	✗	✗	✗	✗
Casisi	min C_{tot}	✓	✓	✓	✗	✓	✓
Weber	min C_{tot}	✓	✓	✓	✗	✓	✓
Mehleri	min C_{tot} & CO_2	✓	✓	✗	✓	✓	✗
Omu	min C_{tot} & CO_2	✓	✓	✓	✓	✓	✗
Buoro	min C_{tot} & CO_2	✓	✓	✓	✗	✓	✓
Morvaj	min C_{tot} & CO_2	✓	✓	✓	✓	✗	✗
Résimont	max NCF	✓	✓	✓	✗	✗	✗
Master thesis	min C_{tot} & CO_2	✓	✓	✓	✓	✓	✓

Table 1.1: Summary of the characteristics of the articles from the literature review.

CO_2 emissions.

1.2 Framework

The aim of chapter 1 was to describe the context of research linked to the implementation of this model. Moreover, a literature review of past studies subject to the same topic was proposed. Before getting to the heart of the matter, it is meaningful to browse the coming sections and their contents.

First, chapter 2 will list and detail the inputs of the model. Then, the equations and objective functions constituting the body of the model will be addressed in chapter 3. It will be followed by a description of the scenarios that will be investigated through chapter 4. Finally, chapter 5 will discuss the results from the various simulations and a conclusion will be built based on that.

Chapter 2

Inputs

This chapter will explore all the inputs that are necessary for the model to operate correctly. The optimisation model takes the year 2018 as a reference. This means that all time related data like climate conditions, electricity prices and renewable productions refer to this particular year. The utilization of each data will be specified and some methodologies will be detailed. Before getting started, more information related to the geographical situation and history of the industrial park will be provided.

The industrial park "Les Hauts-Sarts" is located in Herstal, a suburban area of Liège. It is the biggest economic center that can be found in the Walloon region, gathering about 460 companies in total. The most represented sectors are the manufacturing industry (37%), corporate services (23%) and business (wholesale trading/automotive industry, counting for 18%) [25]. A complete chart containing all the sectors and their proportion is displayed in FIGURE A.1 of APPENDIX A. Historically, the industrial area was created in the 1960s and expanded its territory throughout the years, becoming more and more important. Today, it extends over 450 hectares and is divided into 3 zones, which are shown in FIGURE A.2 of APPENDIX A. In the future, a plan to construct a fourth zone has been launched. A lot of other projects are investigated such as the development of a micro-grid, in which the University of Liège is involved [26].

2.1 Structure of the network

2.1.1 Nodes and Edges

The structure of a district heating network is composed of nodes and edges. In this work, nodes are assumed to be the locations where energy is produced and consumed, while edges are used to distribute heat to the end-users. Nodes are thus the only places that can accommodate a heat or a power installation. Three types of nodes are defined in this model. First, the nodes can be *centralised*, which correspond to zones that are free from construction, on which large heat or power plants could be built. Centralised nodes are represented in **red** in FIGURE 2.1. Then, nodes can be *decentralised*. The latter correspond to the companies of the economic park that accepted to be part of the project and to give some data about their heat and electricity consumption. Companies play the role of prosumers as they exchange both heat and electricity with the DHN and the grid respectively. These spots are represented in **dodger blue** in FIGURE 2.1. The last type of nodes coincide with street intersections. They are pictured in **black** and aim at forcing the pipes to follow the roads.

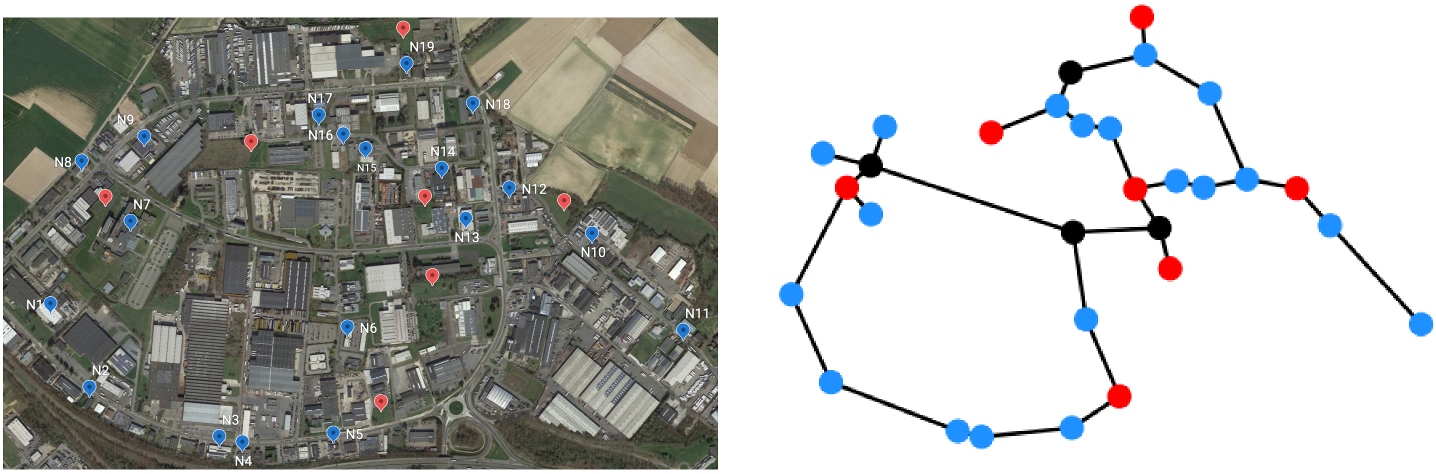

(a) Satellite image of the industrial park (b) Potential grid for the heating network

Figure 2.1: Two representations of the industral park "Les Hauts-Sarts".

As can be seen in FIGURE 2.1(a), the only zone of the industrial park to be studied is zone 1 because the great majority of data files did belong to this part of the map. Moreover, it regroups most of the activities of the entire site. A list of the companies and their annual energy demands is given in TABLE 2.1. Their locations in the satellite image can be found by identifying the matching node number in the table.

Concerning the edges, they are represented as **black** lines in FIGURE 2.1(b). In this layout, the maximum potential connections between all the nodes are displayed. Note that one edge implicitly takes a supply and return pipe into account but a unique one is pictured for the sake of clarity. The optimisation problem will later show which links are actually kept in the final network and in which direction will the water flow (only one circulation possible). The edges have to follow the existing streets in order to be realistic. Nevertheless, being in an industrial park and not a city often allows the pipes to pass through empty fields in order to have a better access to some buildings.

2.1.2 Parameters

An input file called `Parameters.csv` adds some precision on the availability of energy sources at the different nodes. In particular, there is the possibility to mention the presence of already installed production plants[1]. For the electricity sector, some data have been provided by ENGIE IMPACT concerning solar panels and wind turbines. Accordingly, the pre-installed peak power as well as the available areas for future PV panels are taken into account for each company. Furthermore, there is only one wind turbine that is already operating and 90% of its power output is auto-consumed by the company NRB (node 7) [27].

[1] Maximum two can be considered per node

Label	Name	Annual heat demand (MWh)	Annual power demand (MWh)
N1	Consolidated Precision Products	750	4540
N2	TRAVELEC	63.28	54.5
N3	RUTTEN	71.26	44.1
N4	LAGOUNE (GESTANET)	62	30
N5	PELZER	79.95	86.7
N6	CAP Multi-services	144.78	411
N7	NRB	970	8790
N8	TEMPCO SA	48.5	30.1
N9	PASTIFICIO DELLA MAMA	292.25	1200
N10	U.P.T.R.	27.5	10.6
N11	ANB RIMEX	74.73	61.1
N12	Les Ateliers de Monsin	230	80.9
N13	FRIANDA	203.32	715
N14	AQUATIC SCIENCE SA	107	93
N15	POMMEE	80	108
N16	SIBLE EXPERTISE	62.43	1.06
N17	NA VISIBLE	30	4.72
N18	GEMACO	71.83	46.9
N19	BELMECA	67.12	23.9

Table 2.1: List of companies included in the project.

For the heating sector, no data were accessible and there is thus no certainty regarding the type of heat source initially established at the nodes. Therefore, it was assumed that the existing heat technologies were outdated and had to be replaced everywhere. In the parameters file, it is also possible to indicate the maximum usable area dedicated to energy production at the companies. As this information was also unspecified, the dimensions were left at sufficient sizes so that they doesn't limit the possibilities in the MILP.

Finally, binary values can be put beforehand to enable/disable the installation of certain technologies at some nodes. A few examples are that future wind turbines and large heat plants can only be constructed at central nodes, which are more convenient for such technologies.

2.2 Heat

2.2.1 Technologies

The potential heat supply sources will be introduced in this section. A particular attention has been given to include a wide variety of heat technologies in order to increase the range of possibilities when the MILP optimises the district network. To do so, several fossil and non-fossil fueled heat productions with various sizes are considered. Moreover, the economy of scale is taken into account for each technology by distinguishing small, mid and large scale installations. Indeed, the real cost functions[2] including scale economies are often represented using the "0.6 rule" [28]. This means that the shape of cost functions is similar to a square root curve and is thus non-linear. So, piece-wise linear functions are used to provide an efficient approximation, which will be discussed in the following sections.

Natural gas boiler

Concerning natural gas boilers, three sizes are considered in the mixed-integer linear program. For decentralised nodes, only small or mid sized boilers are possibly installed due to space limitations. Alternatively, large sizes can be potentially established at central nodes. The investment costs were retrieved from [29,30] for specific capacities. Some articles in the literature review did use such data and designed a DHN based on predefined capacities. This limits considerably the extend of possibilities in the optimal configuration. Therefore, a regression has been performed so that the program is free to choose any capacity size.

FIGURE 2.2(a) shows a non-linear regression, which represents the real curvature of the cost function. In fact, the cost varies with Capacity$^{0.8}$, which is not so different from the "0.6 rule". Then, FIGURE 2.2(b) represents a piece-wise linear approximation that will be used to keep the linearity of the model. It can be seen that each linear function has at some point the lowest value. Therefore, the MILP is able to pick the best related investment cost at a particular capacity by using binary variables. The way to do that will be specified in chapter 3. For instance, at high capacities, the model will choose the investment cost corresponding to the red line because it is the lowest and most realistic one as it is close to the non-linear curve.

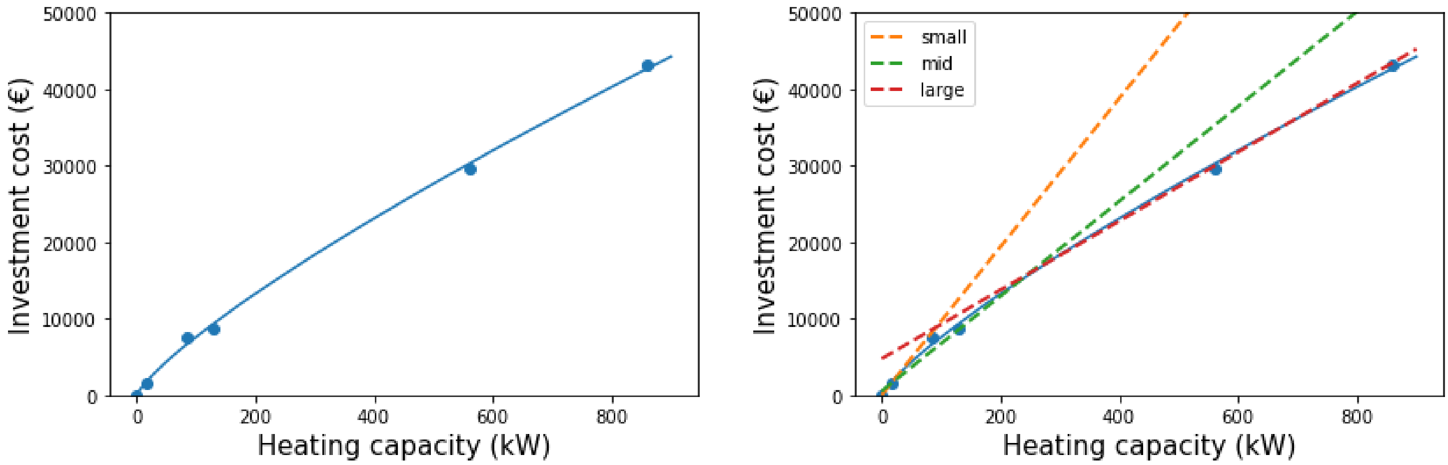

(a) Non-linear regression curve (b) Piece-wise linear regression

Figure 2.2: Regression curve and piece-wise linear function for the investment costs of natural gas boilers.

CO_2 emissions and required specific areas are assumed to be equal for all sizes of natural gas boilers. However, the costs of heating are different as the efficiencies change with the capacity. The values are listed in the two columns referring two natural gas boilers in TABLE B.1 of APPENDIX B. Finally, natural gas boilers can supply

[2]Cost in function of installed capacity.

heat at various levels of temperatures and are thus considered in every simulation discussed in chapter 4.

Combined heat and power plant

Regarding combined heat and power plants, three distinct biomass-fueled technologies were inspected. Two of them provide heat at high temperatures (+90°) and will be studied in the first scenario of chapter 4. The two technologies are a combustion based biomass chp using an organic rankine cyle (ORC) and a gasification based biomass chp using DD-GasE. The latter uses wood chips/pellets, straw and other organic matter to produce a syngas, which is then burnt to produce heat and electricity. This heat is recovered from the cooling circuit and from flue gas cooling.

There are two justifications for examining both types of high-temperature chp plants. First, because they don't operate at the same level of power output. In fact, biomass ORC usually correspond to large sizes and gasification based plants function at mid sizes [31]. This can be viewed in FIGURE 2.3, in which the upper pair of dots corresponds to combustion chp data, whereas the lower pair comes from gasification chp data. In contrast to the gas boiler case, the non-linear regression curve in FIGURE 2.3(a) doesn't represent the evolution of a single technology. Hence, the curve has been plotted to show the tendency of scale economies for a generalized biomass chp plant but actually regroups information from two types of operation. Still, a piece-wise linear function has been elaborated in FIGURE 2.3(b) so that the MILP has the choice between a wide range of capacities.

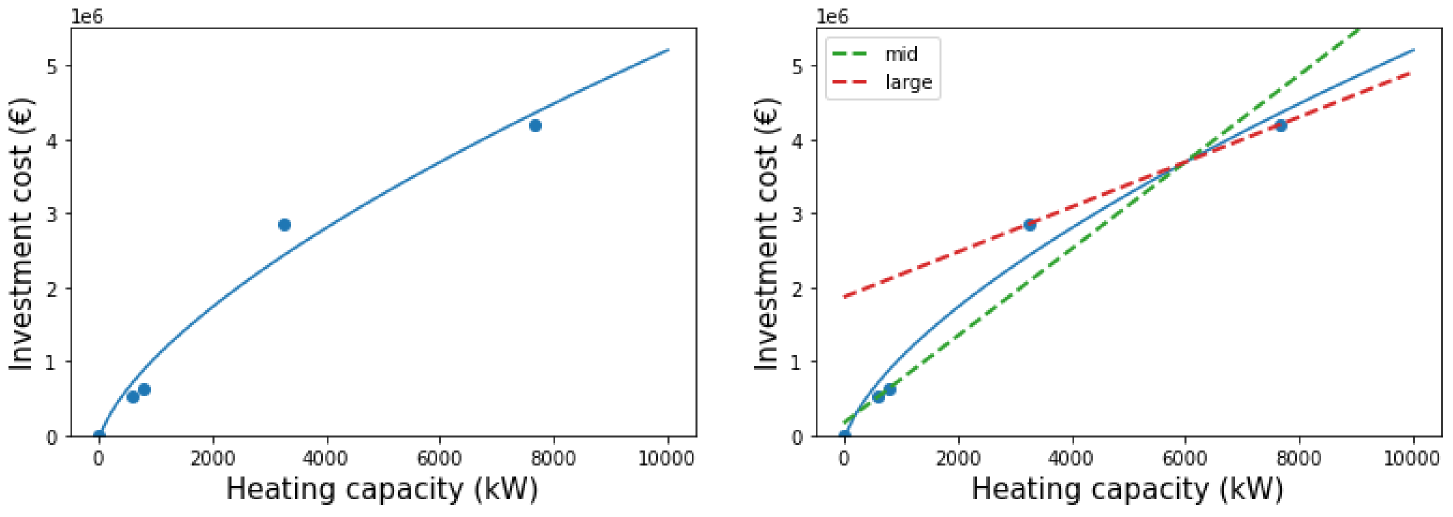

(a) Non-linear regression curve

(b) Piece-wise linear regressions

Figure 2.3: Regression curve and piece-wise linear functions for the investment costs of high temperature chp plants.

Then, another reason to consider both biomass technologies is that they have different thermal and electric efficiencies, which are assumed constant for each type. It can be seen in TABLE 2.2 that gasification chp is better regarding the production of electricity than the combustion chp. But, it has a lower overall efficiency, which is the sum of both efficiencies. Therefore, there is a trade-off between higher overall efficiency and higher electric efficiency. For example, a district with much more

	gasification chp	combustion chp	Stirling engine
ϵ_{el}	0.275	0.14	0.105
ϵ_{th}	0.362	0.72	0.755

Table 2.2: Efficiencies of the three chp technologies.

electric demands than heating ones and with high electricity prices would probably prefer a gasification chp. Other information concerning the cost of heat, greenhouse emissions and specific area can be found in TABLE B.1 of APPENDIX B. The two technologies have similar operational costs found in [32] and are assumed to have equivalent specific areas. They differ however in their CO_2 emissions, computed for complete life cycles of large scale biomass chp (combustion and gasification) in [33].

As mentioned at the beginning of this section, a third type of chp plant was investigated, which is the Stirling Engine. It operates at small/mid ranges around 250 and 500 kW of useful heat output and is fueled with biogas. The same way it has been done for previous technologies, a regression method has been used to obtain a linear function for the investment cost. It is very similar to the one retrieved for a mid size biogas chp in FIGURE 2.3(b). Moreover, Stirling engines are able to supply heat at lower temperatures (+70°) [34] and will thus be used in another scenario, in which the impact of lower temperatures are analysed. As shown in TABLE 2.2, a drawback concerning Stirling engines is that they have low electric efficiencies. Extra information can be found in TABLE B.1 of APPENDIX B. In particular, this type of chp has higher costs of heating and the same CO_2 emissions as gasification chp was assumed because it also uses biogas.

Finally, the potential locations for each type of chp technology are the central nodes. First, this has been assumed because of space limitations inside companies. Moreover, a lot of PV panels are already placed on roofs. This means that firms already produce a certain amount of their electric consumption and the power output from a chp plant would therefore not be so beneficial as they would only work as back-up generators. Lastly, considering large plants at central nodes would able to take advantage of economies of scale.

Heat pumps

The last heating technology to be considered is the air-water heat pump. In this thesis, small and mid capacities are analysed and can be installed at any company. Accordingly, large central heat pumps at central nodes are not considered. The industrial integration of large scale heat pumps was studied by SCHLOSSER *et al.* [35]. The article emphasized the importance of cooling demands for industrial processes in addition to the heating demands. It concluded that large capacities HP are well suited and of great benefit when both heating and cooling are needed. As only heat loads are taken into account for the industrial park, it was decided not to add large heat pumps. Geothermal heat pumps were neither envisaged in the MILP problem. Some reasons are listed in [36] such as intensive investment costs or the decay in the supply heat from the ground source heat pumps after one or few decades.

The way air-source heat pumps were integrated in the model is similar to the previous technologies. Data were retrieved from a manufacturer's brochure, which comes from the company OCHSNER in this case [37]. Several prices and power outputs related to the same heat pump model were used to construct the regression curve in FIGURE 2.4(a). Then, a piece-wise linearisation is effectuated in FIGURE 2.4(b) to keep the model linearly solvable.

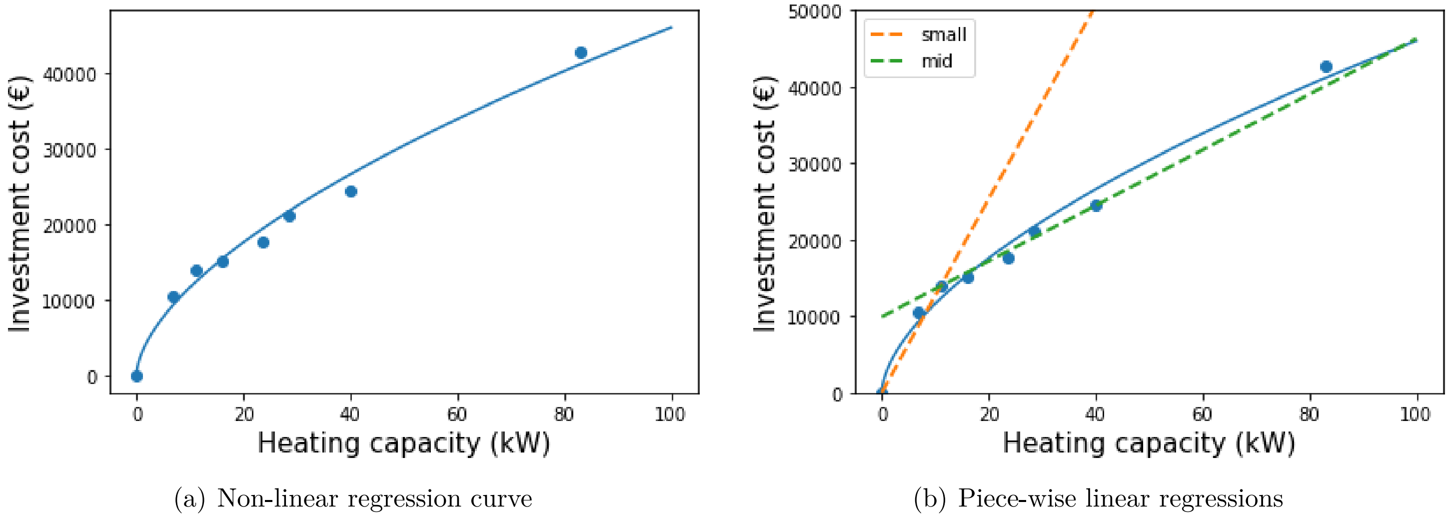

Figure 2.4: Regression curve and piece-wise linear functions for the investment costs of heat pumps.

As for the other devices, additional information is disposable in TABLE B.1 of APPENDIX B. Note that the cost of heat is not fixed in advance for heat pumps. Indeed, it depends on the electricity price and the COP at a certain hour of the year. The way it is modeled will be detailed in chapter 3. In short, if some heat pumps are installed, their heat production is considered as an electrical load, with the coefficient of performance being the conversion factor between the two terms. Therefore, the COP needs to be established on an hourly basis. This has already been computed in the initial model of the University for actual heat pumps working at an output temperature of 90°C. In chapter 4, simulations for different heating temperatures will be studied so additional COP curves for 70°C and 50°C have been calculated. The three curves are shown for a winter and a summer period in FIGURE 2.5. First, it is easily observable that the coefficient of performance increases with outdoor temperatures at the evaporator. Then, the COP values for 90°C and 70°C are really close, while they are much higher at 50°C. This has been investigated in a number of articles. The graph in FIGURE B.1 of APPENDIX B shows a general trend for heat pumps, in which a similar evolution of COP values for different condenser temperatures is plotted.

The hourly COP values obtained for different temperatures are assumed equal for all the capacities. This approximation simplifies the problem and suggests that the coefficient of performance is mostly influenced by the temperatures at the evaporator and the condenser, which are the same for all sizes.

Thermal storage

Thermal storage devices are essential in future generations of district heating networks. GUELPA *et al.* [38] reviewed some advantages and disadvantages of integrating them in the energetic mix. Primarily, thermal storage installations reduce investment and operating costs. This is achieved because they enable to reduce the

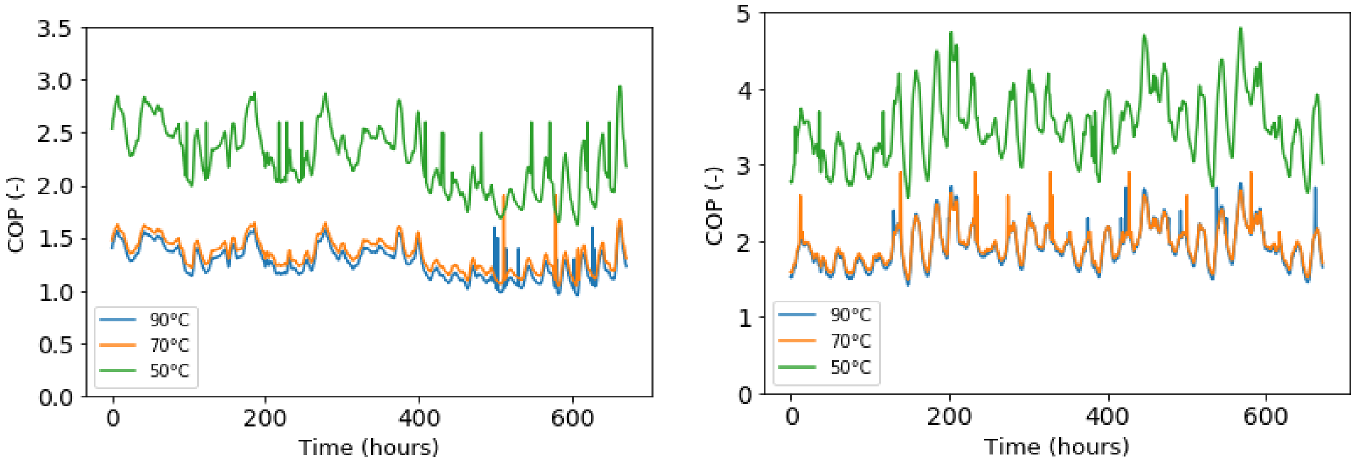

(a) COP values in February 2018

(b) COP values in July 2018

Figure 2.5: Regression curve and piece-wise linear functions for the investment costs of heat pumps.

size of some power units and flatten the thermal peak loads. Other aspects are investigated in the article but overall, thermal storage increase the efficiency of a district heating and therefore they are environmentally and economically beneficial.

Three types of storage technologies exist and are also detailed in [38]. The most common and widely used in district heating systems is the sensible heat thermal energy storage (SH-TES). As the name suggests, the increase and decrease of the storage medium's temperature serves to store heat. Water is usually used as storage fluid because it is cheap and has desirable thermal properties. Moreover, it makes it possible to have a direct connection with the water flowing in the pipes of the district network. Then, latent heat storage is another type of system, which uses the phase transition of a material to store thermal energy. It enables to store energy at a constant temperature but requires more complex regulation of temperature variations during operation. Lastly, chemical energy storage are possible technologies that either use reversible chemical reactions or adsorption/absorption to store heat.

In this case, short-term SH-TES using a water tank is the kind of technology that has been studied. This decision is supported by the fact that SH technologies have the lowest costs and are the easiest to operate, which makes them so popular. In the optimisation program, thermal storage plants can only be installed at centralised nodes as a huge volume is needed. Additional information about the investment cost and the energy density is available below. The operation costs are very low in practice and are often neglected in the literature.

Investment cost (€/kWh)	Operational cost (€/kWh)	Energy density (kWh/m^3)
2	0	50

An example of such storage tanks is shown in Figure 2.6. In this picture, the respective volumes are 2000 m^3 for the left tank and 5000 m^3 for the right one. Regarding the potential free area available at the central nodes of the industrial park, an upper size limit has been fixed such as installed tanks can not be bigger than 2000 m^3. This corresponds to a capacity limit of 100 MWh. Finally, the storage technology functions at any temperature level so it can be included independently of the supply and return temperature designs in a district heating system.

Figure 2.6: Two thermal storage tanks combining for a capacity of 400-500 MWh.

2.2.2 Heat consumption

Annual data

Generally, heating demands in buildings are composed of space heating and hot domestic water. The latter has been neglected because the case study only consists of industrial or office buildings. As already mentioned, the heating sector lacked some data about the existing technologies and the consumption of the companies. Indeed, the annual electricity demands in TABLE 2.1 were given for all the companies but for heating, only 9 companies[3] provided their annual consumption. Hence, half of the yearly values had to be computed using a regression. To do so, two options were investigated. Originally, a regression between the yearly heating consumption and the area of the corresponding companies was sought. The areas would be easily recoverable from GOOGLE EARTH. Though, the results were not satisfying and may be due to the fact that the captured areas didn't reflect the actual space that is being heated. To improve this, it was decided to rely on verified data to construct the regression. To do so, the annual heat data have been put in relation to the electrical ones. Physically, it also makes sense as the level of consumption refers to a level of activity and operating this way keeps the relation between the energy demands consistent.

FIGURE 2.7 illustrates the regression that was used to find the lacking data for yearly heat demand. It can be observed that the regression curve forms a proper approximation of the lower and higher values. Besides, two tendencies can be retrieved from these plots. Indeed, smaller companies with lower energy demands tend to have a higher proportion of heating demand than power. This is observable in FIGURE 2.7(b), where most of the points are above the "Power=heat line". FIGURE 2.7(a) shows exactly the opposite trend for bigger companies. A reason for that

[3]Consolidated Precision Productions, Aquatic Science SA, Lagoune (Gestanet), Les Ateliers de Monsin, NRB, Pommee, Travalec, U.P.T.R, NA Visible.

could be that big companies need more electric power for potential data centers or to make some machinery work.

In fine, the building heating demands that will be given as inputs to the mixed-integer linear program are not those described in this section. In fact, the program is a multi-period optimisation model, meaning that a single annual value is not what is required. Instead, hourly load profiles will be employed. Nevertheless, these profiles are derived from the yearly consumption and it was thus necessary to introduce the latter data correctly.

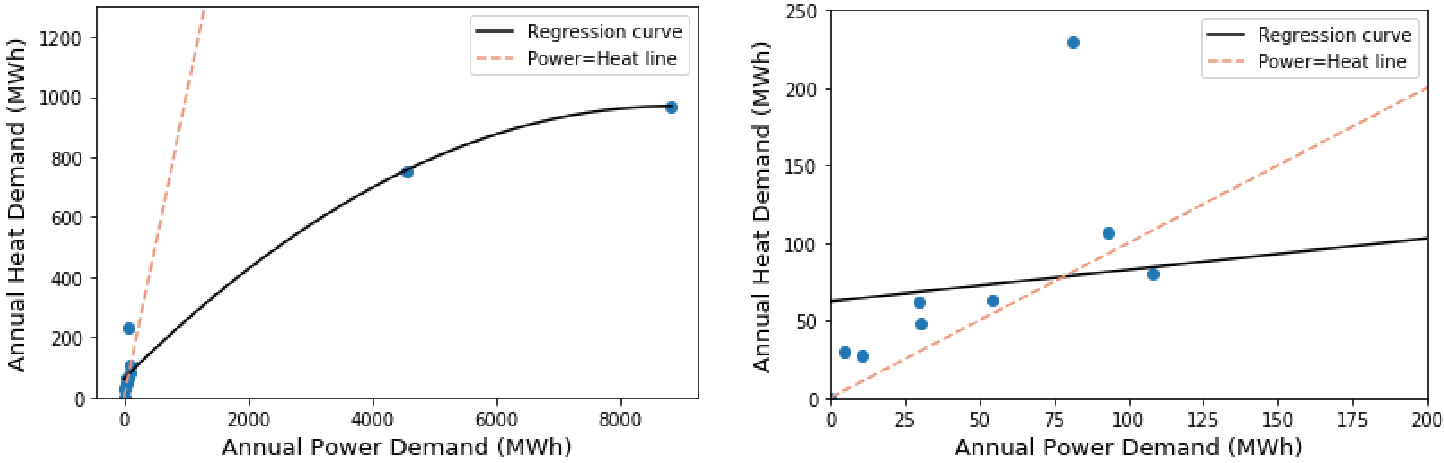

(a) Regression between input data (b) Zoom on lower values

Figure 2.7: Regression curve and equal heat/power consumption line.

Hourly load profiles

Many methods exist to model the heat loads in different types of buildings. Still, these methods can be distinguished into two major families. The first one to be considered is the *bottom-up approach*. This approach applies simulation models to predict future heat loads as well as indoor and outdoor environmental conditions [39]. Some examples of software are EnergyPlus, TRNSYS or TEASER and they all have similar procedures. Diverse information such as building archetype, construction data, thermal mass and usage schedules are asked beforehand. Then, thermal models are constructed based on the inputs. They are implemented in equivalent R-C electric networks to describe heat transfers and storage. The name *bottom-up* refers to the methodology, which starts with individual building data and finally obtains heat load profiles for a whole neighbourhood. The advantage of such *bottom-up* techniques is that they are based on physical models, which take thermal inertia into account. This in turn makes it possible to predict some complex cases like peak demands at certain periods. However, this approach is hard to establish as a lot of knowledge related to the structure and heat audit are required. Consequently, the *bottom-up* procedure is well suited at the design phase for future buildings or when considering renovation measures, but less for existing constructions [40]. Adding to that the lack of information concerning the thermal and material properties of the buildings in the industrial park, and it resumes why the *bottom-up* approach was not used.

The other method for estimating load patterns is the *top-down* approach. The mechanism is opposite to the previous one. Here, one starts with regional heat energy demands, which are then subdivided into all the existing buildings and all the periods. One way to perform *top-down* analysis is by evaluating historical data and statistics. This was studied by LINDBERG *et al.* [41], in which a *top-down statistic* regression model based on hourly monitored data from hundreds of non-residential buildings in Norway was implemented. The result is a parametric function that returns the energy signature in kWh/m^2 for a number of building types and representative days, weeks and years. The only required inputs are outdoor temperatures and floor areas. The pros of this method are that it is easy to carry out as only a few inputs are needed. In addition, the load patterns are derived from measured data, which is a proof of reliability. But, this method have troubles to capture some dynamics as no thermal inertia is considered. As a consequence, the load profiles are said to be aggregated or smoothed and don't represent qualitatively the peak loads. Moreover, the approach can neither recover load profiles for other archetypes of buildings than the one considered in the data samples and no future renovations can be analysed. In this case, only existing constructions are involved in the MILP problem, making this alternative for computing the profiles an interesting option. Nonetheless, not enough statistical studies were found for Belgium and for industrial buildings so statistical procedures were not used to retrieve the hourly heating patterns for the companies of the industrial park.

The way the profiles were obtained is still similar to a *top-down* approach as they are based on given consumption data. The latter to be used are the annual heat demands presented in section 2.2.2. The methodology that has been employed estimates the rate at which buildings loose heat, which in turn gives the corresponding heat loads. The method was suggested by GUILLEMOT *et al.* [42] for a district heating system in France and results showed that the mean average proportional error between the computed and the measured values are within ± 15%. An overview of the computation process is demonstrated hereunder.

The primary assumption is that the building hourly heating capacity is proportionally distributed with respect to the temperature difference between the inside set point temperature and the external temperature. In other words, the bigger the difference in temperatures between inside and outside, the higher heat consumption will be required. A general expression of the hourly heat loads is observable at EQUATION 2.1 :

$$\dot{Q} = C * DH \tag{2.1}$$

Where $\dot{Q}$ and DH are respectively the hourly heating load and the heating degree hour. Next, C refers to the building thermal capacity. The latter can furthermore be detailed as :

$$C = \frac{E_{year}}{DH_{year}} \tag{2.2}$$

In EQUATION 2.2, E_{year} represents the annual heating consumption of a building and DH_{year} corresponds to the sum of all the heating degree hours throughout a year. LI *et al.* [36] defines the concept of heating degree hours as by how much and for how long (in hours), outside air temperature is lower than a base temperature, also called set point temperature. There are thus two aspects in the definition, a quantity and a time. In this case, the period is specified to be one hour. Then, concerning the value of the difference in temperatures, this highly depends on the choice of the set points and the type of day. Hence, for working days, the inside set point temperature has been put to 20°C for working hours (7-19h) and to 15°C for non-working hours [43]. In order to keep the representation as much realistic as possible, heat demand only appears when the difference with the set point is higher than 1°C. This way, situations in which heat loads correspond to very little temperature differences are avoided. During the weekend, no heating degree hour is added and no heat load is considered. The hourly outdoor temperatures for the year 2018 have been used to compute the temperature differences with the set points. When all the heating degree hours are calculated, they can be summed to obtain the DH_{year} variable in EQUATION 2.2. Finally, C is fixed and $\dot{Q}$ for each hour can be computed having the corresponding heating degree at each hour. $\dot{Q}$ is found similarly as a weighted sum, where the weights are the degree hours, dependent on the outside temperatures and the week schedules. The plot representing the hourly heat load estimations of the company NRB is represented in FIGURE 2.8. It is clearly observable that the consumption is lower during summer and higher during winter. Additionally, the null demands at the weekends can be viewed in this plot.

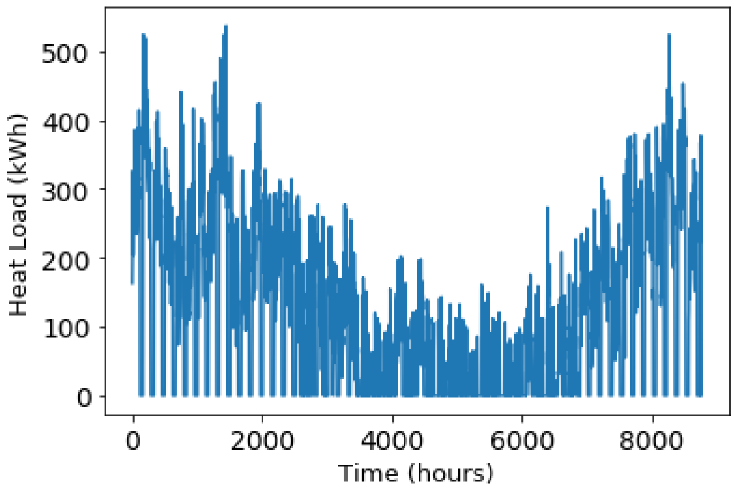

Figure 2.8: Heat load profile for the company NRB.

2.3 Electricity

2.3.1 Technologies

Two renewable technologies are included in the model, which are photovoltaics and wind turbines. For both of them, most of the data have been provided by ENGIE IMPACT, which developed a program called `Prosumer`. This program aims at optimising the installation of PV panels and wind turbines without considering heat demands but focusing on in-depth economic aspects. The input files contain the amount of installed photovoltaics at each company and the potential for future installations. This means that the MILP can choose to install any size of photovoltaics until it reaches the maximum bound permitted by the area of the building's roof. Analogous information for wind turbines are also available in the data files.

The different inputs related to both renewable technologies are shown in Table 2.3. Concerning solar panels, no company had a higher PV potential than 250 kW so the investment and operating costs have been taken for this range of capacities. Regarding wind turbines, it is not realistic to consider any size to be installed at a central node. Indeed, manufacturers like VESTAS propose a catalog with fixed outputs and it is not scalable to any wanted power. For this reason, wind turbines are the only technology in the optimisation problem to have a pre-defined capacity. The latter has been set to 2.2MW such as the wind power installed at NRB. The required area is also mentioned for each technology [44, 45].

	PV (0-250 kWp)	Wind (2.2 MW)
Investment cost (€/kW)	740	1000
FO&M costs (€/kW/year)	10	22.73
Required area (m^2/kW)	5	1.5

Table 2.3: Investment and operational costs for PV panels and wind turbines.

Renewable production

In general, modelling the electric productions of renewable sources necessitates to know some climatic data over the year. For instance, computing photovoltaics production would require the hourly irradiation at a specific location. For wind turbines, one needs to know the hourly wind speed. The latter would then be used in a cubic function relating power and wind speed and it would have to be linearised in this case. Fortunately, the data files from ENGIE IMPACT also comprise measurements of the specific produced electric power for on-site PV panels and wind turbines for the year 2018. As measured data will always be faithful to reality and that no linearisation has to be done, this will be used to form the energy production coming from renewables during the year 2018. For both photovoltaics and wind turbines, two curves representing their productions over one week in February and another in July are shown in Figure C.1 of Appendix C. The distinction between winter and summer productions for solar panels is clearly observable in Figures C.1(a) and C.1(b). Conversely, the stochastic behaviour of wind power is particularly visible in Figures C.1(c) and C.1(d). Note that productions below 0.01 $\frac{kWh}{kW}$ were replaced by 0 for numerical purposes[4].

2.3.2 Electric consumption

Unlike heat load profiles, for which either an energetic audit or a model of the building has to be effectuated in order to estimate the consumption, electric load patterns are easily measurable. These measures were also provided in the data files from ENGIE IMPACT. Yet, the loads were given on a quarter-hour basis so a mean was computed to obtain an hourly basis. The electric consumption profile for a company is shown in Figure 2.9. Around hour 5000 (end of July), there is a drop in the electric consumption, which is probably due to a holiday period for the company.

[4]The reason is to reduce the range of the matrix of coefficients as much as possible.

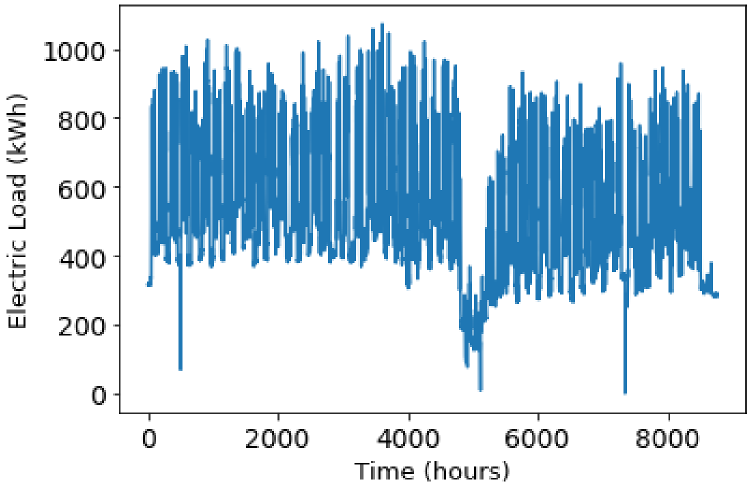

Figure 2.9: Electricity load for the company Consolidated Precision Products.

2.3.3 Electricity price

The same way the cost of heat has been presented in a previous section, the price of electricity needs to be clarified. In the data files received from ENGIE IMPACT, the peak and off-peak electricity prices for each company are mentioned. The amount to be paid for electricity bills was found to be very different from one firm to another. As an example, FRIANDA SA has a contracted peak price of 0.109 €/kWh whereas it reaches 0.235 €/kWh for PELZER SA. As expected, the electricity costs greatly depend on the size/consumption of each consumer. Therefore, three synthetic price curves on an hourly basis have been built for small, middle and large sized companies. This way, it will make the results more realistic and some particularities in the optimal solution may appear, that would not be the case if the same electricity price was chosen for every enterprise.

A review of several consumer profiles has been directed by the CREG and the VREG in [46]. A list of the different consumers is displayed in FIGURE C.2 of APPENDIX C. Based on the annual electric demand shown in TABLE 2.1 of SECTION 2.1.1 and the profiles of FIGURE C.2, all the businesses have been classified in function of their consumption. According to [46], two of them had an industrial profile of more than 2000 MWh annually and three had the profile of a small professional firm with more than 160 MWh a year. The remaining companies are grouped together and have an annual consumption above 30 MWh.

After the consumer profiles have been established, the hourly electricity price for each type has to be constructed. As a reminder, in Belgium and other European countries, the electricity bill is composed of three components when referring to companies. First, there is the commodity price, which is attributed to the price of the produced energy. Then, the network costs for the distribution of energy has to be added to the account. Lastly, another cost in which PSOs[5], taxes, levies and surcharges are grouped together is included. In this category, some costs are on the federal level and others are on regional levels, meaning that it can differ between belgian locations and so it is important to search for data related to the Walloon Region. TABLE C.1 of APPENDIX C resumes the proportions, retrieved from [46],

[5]Public Service Obligations

for each component of the bill explained above. It can be seen that the bigger the company, the higher the fraction of the commodity component in the total price. This means that less additional costs have to be disbursed, leading to an overall lower costs for large corporations. The resulting electricity prices for a summer and a winter period are plotted below in Figure 2.10.

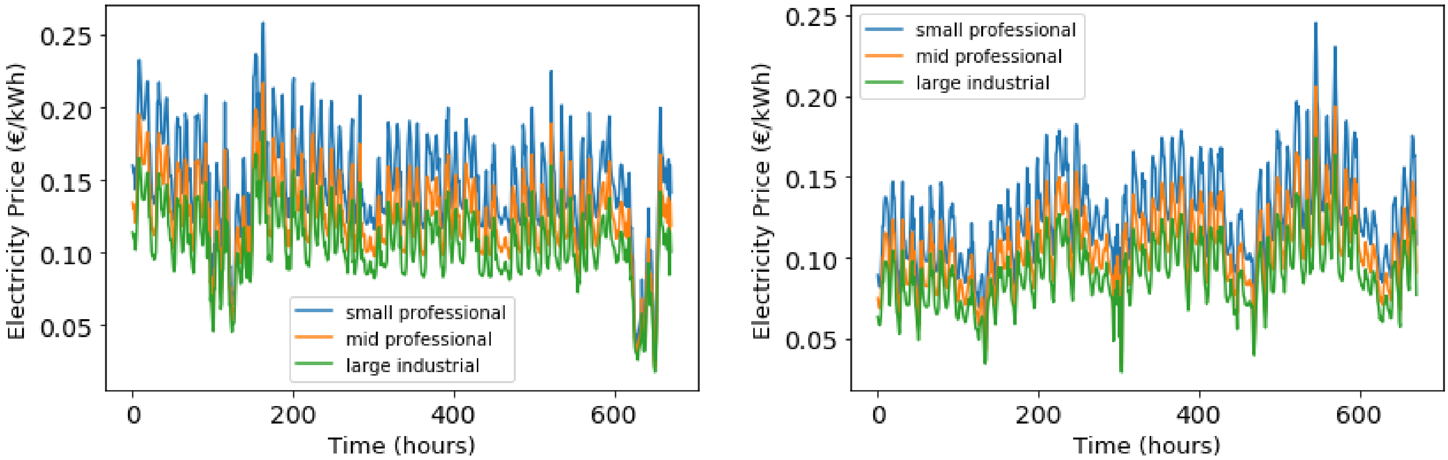

(a) Resulting prices for February 2018

(b) Resulting prices for July 2018

Figure 2.10: Electricity prices for two months and for the three established profiles.

2.4 Other costs and subsidies

This section aims at giving some information about costs related to other components of the DHN and at introducing the subsidies that were envisaged for the MILP problem. The mathematical developments to obtain the different cost functions and regressions can be found in [24].

2.4.1 Costs for diverse components

Cost of pipes

In brief, the methodology starts by expressing the diameter of the pipes as a function of the maximum power flowing in them. This function $D_{pipe} = g(P_{max})$ is highly non-linear. After, a first regression $Cost_{pipe} = f(D_{pipe})$ using price data for pipes is computed and can be viewed in Figure D.1(a). Then, combining both functions gives $Cost_{pipe} = f(g(P_{max}))$, which is the solid line plotted in Figure D.1(b). In this same figure, two other dotted-lines represent the initial regression made in [24] and another one used in this model. They are very different because the regression was not made on the same range of maximum power flows. In fact, in the original model, the limit in the pipes' capacity was put to 1000 MW. In this case, the overall heat consumption are much lower and maximum flows reached a peak around 20MW. Therefore, the heat losses were underestimated and new costs have been calculated. Moreover, a distinction between outer and inner city pipes was studied in the article but only the outer city case has been maintained in this work. The pressure losses in the pipes have in turn been fixed to 100 Pa/m, as explained in [24].

Heat losses

An analytical model of the heat transfers between the supply and return pipes as well as with the outdoor environment was built. FIGURE 2.11 shows the electric-equivalent circuit used for the thermal model. A first result obtained in [24] was that heat losses per unit length are not so dependent on the power flow but much more on the diameter of the pipes.

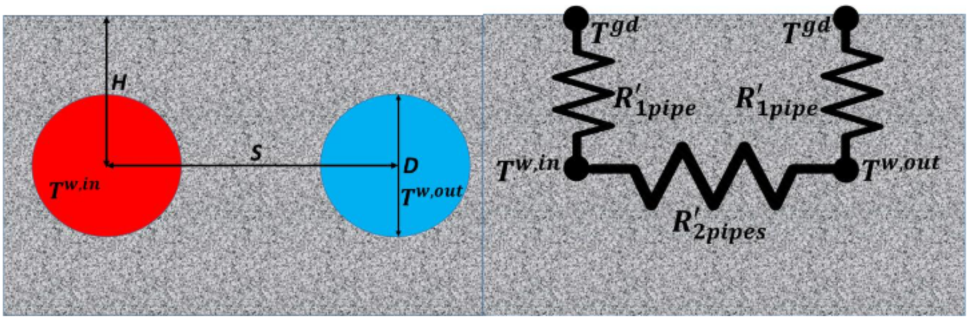

Figure 2.11: Heat transfer model for heat losses in pipes [24].

Consequently, after having computed some points linking heat losses to diameters, an interpolation $Heatlosses = f(D_{pipe})$ is applied, as shown in FIGURE D.2(a). Then, the same previous relation $D_{pipe} = g(P_{max})$ is used in order to express heat losses per unit length as a function of the maximum power flow : $Heatlosses = f(g(P_{max}))$. Similarly to the costs of pipes, the losses have been computed for lower values of maximum power flow and the result for supply temperatures of 90°C is plotted in FIGURE D.2(b). In the approach, thermal losses are thus dependent on the maximum flow but also on the level of temperature.

In the initial model of the University, the supply and return temperatures were fixed at 90°C and 60°C respectively. Because this thesis has the willingness to propose a 4^{th} generation district system functioning at low temperatures, the heat loss computations were all re-implemented for design temperatures of 70-40°C and 50-20°C. These three test cases with different temperature levels will be detailed and studied in chapter 4. Lastly, heat loss coefficients for thermal storage were also calculated.

Substation

Finally, the cost for installing a substation at each end user has to be settled. In [24], one substation was installed per street as the consumption were taken edge per edge. This is not the case in this work as one substation will be installed at each connected company. So, different prices have to be considered. On the market, two types of substations exist. First, the connection can be indirect, meaning that the primary and secondary flows are separated by a heat exchanger [47]. Then, connections can also be direct, meaning that the same flow heats the building and no heat exchanger is needed. Both systems are widely used and the costs retrieved from the DANISH ENERGY AGENCY show that prices don't differ much between the two types of connections. Economies of scale were observable thus a regression was carried out. The price for substations covers the costs of all valves, controllers, filters and pumps that are necessary for the operation [8]. In this case, the connections are indirect and thus need a heat exchanger at each node that is connected to the heating network.

2.4.2 Subsidies

Depending on the belgian region, different supporting schemes are proposed by the government. In Wallonia, financial assistance can be provided in three ways [48]. First, green certificates can be granted for renewable energy sources. The number of quotas is proportional to the produced electricity from the installation. These certificates can then be sold to electricity suppliers such as ELIA, who are obliged to purchase a certain quantity of them each year. The technologies concerned by this measure are wind turbines, solar panels, biomass/biogas chp and hydro-power plants.

The second supporting action led by the Walloon Region relates to the investment costs borne by companies in renewable sources. The subsidy is computed based on the extra costs required for the installation of renewable technologies compared to fossil-fueled ones at the same capacity. The amount of perceived money depends on the size of the firm. For large companies in a development zone of the province of Liège, the gross rate is 25%. This ratio is then multiplied by the additional cost for buying a renewable energy plant, which finally gives the amount of the subsidy [49].

The last aid is called net-metering. As the name suggests, the principle is to measure the electric energy taken from the grid and injected into it. Regarding the net value, a compensation is granted to the prosumers. This will be further detailed in chapter 3 as well as the support for investment costs. However, green certificates were not added to the model because the policies regarding the amount of the subsidy and the necessary conditions tend to change frequently, which makes it difficult to model.

Chapter 3

Model

A general form of an optimisation problem is shown below. Three different elements compose such numerical problems and will be detailed in the next sections. Firstly, the goal of the optimisation is to minimize or maximize an objective function. In the given example, the function *f()* is the **objective function** and the aim is to minimize its value. This function is subject to a set of **constraints**, corresponding to *g()* and *h()* that have to be respected. The objective and the constraints depend on **decision variables** represented by x hereunder.

$$\begin{aligned} \underset{x}{\text{minimize}} \quad & f(x) \\ \text{subject to} \quad & g_i(x) \leq 0 \quad , \; i = 1, \ldots, n. \\ & h_j(x) = 0 \quad , \; j = 1, \ldots, p. \\ & x \in \mathbb{R}^N \end{aligned}$$

When a value of the objective function *f()* satisfies all the constraints, the solution for x is said to be feasible. Among all these feasible solutions, the program searches for the optimal one. When the problem formulation is linear or at least convex, the optimal solution is always unique, which is not the case for non-linear problems. The latter ones often find solutions that are optimal locally but nothing guarantees that it is the best one possible. This is a reason why linearity was preserved in this model by making linear regressions on some functions. However, it is important to note that some precision is lost when linearising real functions. There is thus a trade-off between fidelity and robustness. Some efforts have been put to maintain this robustness and approximate at best the non-linear behaviours. For instance, piece-wise linear functions have been employed to approach the real functions. In this work, the category of optimisation problem that is used is called mixed-integer linear programming. The particularities and the components of this type of programming are further explained in the following sections.

3.1 Variables

The specificity of mixed-integer programming is that different sorts of variables are considered. Indeed, the variables can either be continuous or binary. These two natures make MILP programs perfectly fitted for the development of an optimal design and operational strategy in a district heating project. In fact, both aspects of the problem have to be optimised jointly because they influence each other.

	∀ nodes/edges	∀ timesteps	∀ Technologies	Domain
Decision variables				
Heat capacity	✓	✗	✓	$\mathbb{R}_+$
Electric peak power	✓	✗	✓	$\mathbb{R}_+$
Storage capacity	✓	✗	✓	$\mathbb{R}_+$
Pipe capacity	✓	✗	✗	$\mathbb{R}_+$
Pipe construction	✓	✗	✗	0/1
Heating network connection	✓	✗	✗	0/1
Installation of heat source	✓	✗	✓	0/1
Installation of wind turbine	✓	✗	✗	0/1
Operational variables				
Heat production	✓	✓	✓	$\mathbb{R}_+$
Heat flows and losses	✓	✓	✗	$\mathbb{R}_+$
District heat dispatch	✓	✓	✗	$\mathbb{R}_+$
Grid interaction	✓	✓	✗	$\mathbb{R}$
Storage interaction	✓	✓	✓	$\mathbb{R}$

Table 3.1: Summary of the variables from the optimisation problem.

Table 3.1 classifies all the variables used in the model. It can be viewed that all design variables are logically time-independent. Some of them are binary and decide whether or not a technology or a grid connection is installed. Others are continuous in the positive domain and indicate the capacity of one technology.

Concerning operational variables, they are all time-dependent on an hourly basis. They describe the operation of the whole district in terms of production, distribution and other synergies. Some model variables have been regrouped in the different classes of the table for more clarity.

3.2 Objective function

The second component in the formulation of an optimisation problem is the objective function. The articles of the literature review mentioned a variety of objectives. Some of them did minimize operational costs only, others considered the total costs and still others envisaged to add CO_2 taxes in their function. In particular, in the original model [24], it was decided to maximize the net cash flow, taking revenues from heat sales into account. In this case, the goal of the optimisation is to minimise the total costs and CO_2 emissions, which are two conflicting objectives. However, instead of dealing with a multiple-objective optimisation, the problem will be reformulated in order to minimize only one function like in [23]. Several methods exist to modify such multiple objectives into a single one. The one being applied here is called the ϵ-constraint method. The idea is to optimise one primary function and to translate the remaining functions into supplementary constraints. The approach is illustrated below :

$$\begin{aligned} &\text{Multi-objective}: \quad \underset{x}{\text{minimize}} \quad C_{tot}(x) + CO_2(x) \\ \Rightarrow \quad &\text{Single-objective}: \quad \underset{x}{\text{minimize}} \quad C_{tot}(x) \\ &\qquad\qquad\qquad \text{subject to} \quad CO_2(x) \leq \epsilon \end{aligned}$$

It can be observed that the total costs have been chosen to be minimized and that the CO_2 emissions are limited in the constraint section. The value of ϵ is modified in order to obtain a trade-off front of solutions, that gives the required costs for each specific CO_2 production. This is the procedure at the basis of the Pareto fronts that will be analysed in chapter 4. Now that the objective function has been introduced, it is necessary to define how $C_{tot}(x)$ has been implemented. The latter is composed of the investment costs (CAPEX), the operational costs (OPEX) and some subsidies.

$$C_{tot} = f_{CAPEX} \cdot CAPEX + f_{OPEX} \cdot OPEX - Subsidies$$

No revenues except some initial investment subsidies have been considered. This has been assumed because revenues are difficult to model reliably through a period of 20 years. Moreover, doing so enables to focus on the estimation of costs for diverse district configurations.

As it would be intractable to consider an optimisation over 20 years, a reference year is chosen at the basis of the problem. In this case, the selected year is 2018 and all input data relate to this period. Having settled the reference year, some tools are needed to scale the results over the duration of the project, which is fixed to 20 years[1]. This is done by using f_{CAPEX} and f_{OPEX}, which are actualization factors. Their roles aim at including the value of money over the duration of the project. For example, instead of simply multiplying the OPEX by the number of years, f_{OPEX} takes economic parameters into account to give a better approximation. In this case, both factors depend on the discount rate r as shown in EXPRESSIONS 3.1 and 3.2. The latter has been fixed to 0.03 in the calculations. Yet, inflation of energy prices has not been modelled. More information regarding the actualization rate and the actualization factors can be found in [24].

$$f_{CAPEX} = (1+r)^{N_{years}} \qquad (3.1) \qquad\qquad f_{OPEX} = \frac{1-(1+r)^{N_{years}}}{1-(1+r)} \qquad (3.2)$$

CAPEX

The capital expenditures or CAPEX correspond to the costs of investment and are accounted at the beginning of the project. The different components of the CAPEX are given in EXPRESSION 3.3. Binary variables are written with greek letters to differentiate them from continuous variables.

$$CAPEX = C_{Heat\ plants} + C_{Renewable\ techs} + C_{Substation} + C_{Pipes} \qquad (3.3)$$

- $C_{Heat\ plants}$ [∀ n in nodes, ∀ te in technologies] :

$$\sum_{n}\sum_{te}(a[te] \cdot (P[n,te] - P_{min}[n,te]) + \delta[n,te] \cdot b[te]) \qquad (3.4)$$

[1]This period correspond to the lifetimes of most technologies in this model.

Where a[te] and b[te] are respectively the slope and y-intercept of the linearised cost functions for each size and each technology that were presented in chapter 2. Next, P[n,te] corresponds to the total installed heat capacity at each node, while P_{min}[n,te] refers to the capacity that was already installed. Finally, δ[n,te] is a binary variable that decides whether a heating technology is installed at a particular node or not.

Expression 3.4 is highly related to other constraints from the model. Therefore, these constraints will be displayed earlier for structural and clarity purposes, but are not part of the objective function.

$$P[\text{n,te}] \geq P_{\text{min}}[\text{n,te}] \tag{3.5}$$

$$P[\text{n,te}] - P_{\text{min}}[\text{n,te}] \leq \delta[\text{n,te}] \cdot \text{Cap}_{\text{max}} \tag{3.6}$$

$$\delta[\text{n,te}] \cdot \text{Cap}_{\text{min}} \leq P[\text{n,te}] - P_{\text{min}}[\text{n,te}] \tag{3.7}$$

To begin with, Expression 3.5 makes sure the total installed power at every node and for every technology is at least equal to the pre-installed heat sources. Then, Expressions 3.6 and 3.7 limit the size of heat plants between Cap_{min} and Cap_{max}. These upper and lower bounds are in general fixed so that they don't restrain the number of possibilities in the district energy system. However, some technologies like biogas chp only exist at mid size capacities and the related constraints are thus more tight. In addition, the combination of Expressions 3.4, 3.6 and 3.7 enables to account the costs for chosen technologies only. Indeed, if δ[n,te] = 0, (P[n,te]-P_{min}[n,te]) is null and the cost expression for that technology at a specific node disappears.

- $C_{\text{Renewable techs}}$ [$\forall$ n in nodes, $\forall$ te_{el} in Renewable technologies] :

$$\sum_{n} \sum_{te_{el}} (c_{\text{invest}}[\text{te}_{\text{el}}] \cdot (P_{\text{elec}}[\text{n,te}_{\text{el}}] - P_{\text{elec,min}}[\text{n,te}_{\text{el}}])) \tag{3.8}$$

As a reminder, solar panels and wind turbines are the two available renewable productions in this work. As discussed in chapter 2, no linear regression was applied for both technologies. Instead, a single investment cost proportional to the size was considered. For this reason, no binary variable was necessary for solar panels. Though, one was still required for wind turbines as the capacities are pre-defined. This is shown in Expression 3.10, in which Cap_{max} has been fixed to 2200 kW. Therefore, either the binary variable γ_{wt}[n]=0 and no wind turbine is installed nor payed. Or, it is equal to 1 at a particular node and it can be installed at a certain amount. Expression 3.9 is equivalent to 3.5 in the case of renewable technologies.

$$P_{\text{elec}}[\text{n,te}_{\text{el}}] \geq P_{\text{elec,min}}[\text{n,te}_{\text{el}}] \tag{3.9}$$

$$P_{\text{elec}}[\text{n,wt}] - P_{\text{elec,min}}[\text{n,wt}] = \gamma_{\text{wt}}[\text{n}] \cdot \text{Cap}_{\text{max}} \tag{3.10}$$

- $C_{\text{Substation}}$ [$\forall$ nd in decentral nodes] :

$$\sum_{nd} ((a_{\text{substation}} \cdot Q_{\text{max}}[\text{nd}] + b_{\text{substation}}) \cdot \beta[\text{nd}]) \tag{3.11}$$

Where $a_{substation}$ and $b_{substation}$ are the parameters of the linear regression representing the cost for district network substations. $Q_{max}[nd]$ is the annual peak load for a company at a decentral node, such that substations are designed taking peak demands into account. Lastly, β[nd] is a binary variable deciding for each building if it is connected to the heating network or not. If yes, the installation costs are added to the objective function. Note that $Q_{max}[nd]$ is not a variable and can thus be multiplied by another variable, which is binary in this case, without causing the expression to become quadratic.

- C_{Pipes} [$\forall$ e in edges] :

$$\sum_{e}((a_{\text{pipe}} \cdot \text{pipe}_{\text{cap}}[\text{e}] + b_{\text{pipe}} \cdot \alpha[\text{e}]) \cdot \text{length}[\text{e}]) \tag{3.12}$$

Once again, a_{pipe} and b_{pipe} are the parameters of the cost function defined in chapter 2. To continue, $\text{pipe}_{\text{cap}}[\text{e}]$ is a continuous variable that describes the maximum power possibly flowing in the pipes. Further, α[e] is a binary variable that chooses whether or not a pipe is constructed at a certain edge. The costs of pipes also depend on the length of each edge as the regression was built using data expressed in €/m.

$$\text{pipe}_{\text{cap}}[\text{e}] \leq \alpha[\text{e}] \cdot \text{Max flow}[\text{e}] \tag{3.13}$$

As explained earlier, Expression 3.13 is an upper bound constraint of the variable $\text{pipe}_{\text{cap}}[\text{e}]$, in which Max flow[e] is fixed beforehand. This constraint also permits to avoid costs when a pipe is not built at an edge,i.e. α[e]=0.

OPEX

The operating expenditures or OPEX cover the costs for operating the energy network and its maintenance. These costs are charged over all the project period, meaning that they are time-dependent. Therefore, if the time span is large, these costs may represent the biggest proportion of the total costs, especially for fossil-fueled energy plants. This explains why it can be economically favourable to pay a higher investment price for a bigger installation, which has smaller operating costs. The various elements forming the OPEX are shown in Expression 3.14.

$$\text{OPEX} = C_{\text{Heating production}} + C_{\text{Elec production}} + C_{\text{Grid interaction}} + C_{\text{Pumping power}} \tag{3.14}$$

- $C_{\text{Heating production}}$ [$\forall$ n in nodes, $\forall$ te in technologies, $\forall$ t in time steps] :

$$\sum_{n}\sum_{te}\sum_{t}(c_{\text{heating}}[\text{te}] \cdot \text{power}[\text{n,te,t}] \cdot \text{weight}[\text{t}]) \tag{3.15}$$

Where $c_{\text{heating}}[\text{te}]$ is the operational cost for each technology presented in chapter 2. The continuous variable power[n,te,t] refers to the power produced by a specific heat plant at each time step and each node. Then, weight[t] is included when representative hours are used. The latter help to speed up the computation time of the model by approximating several time steps into a single one, which is multiplied by a weight. Additional information will be provided in chapter 4.

The same way it was done for CAPEX expressions, some related constraints will already be shown in this section. EXPRESSION 3.16 guarantees that the produced power by the heating technologies can never be higher than the installed capacity. A minimum part load of 50% was envisaged for chp plants in EXPRESSION 3.17. This takes into consideration some technical limitations and the fact that chp efficiencies are almost constant above this level [23].

$$\text{power}[\text{n,te,t}] \leq P[\text{n,te}] \tag{3.16}$$

$$50\% \cdot P[\text{n,chp}] \leq \text{power}[\text{n,chp,t}] \tag{3.17}$$

- $C_{\text{Elec production}}$ [$\forall$ n in nodes, $\forall$ te_{el} in Renewable technologies] :

$$\sum_{n} \sum_{te_{\text{el}}} (\text{FO\&M}[\text{te}_{\text{el}}] \cdot \text{P}_{\text{elec}}[\text{n,te}_{\text{el}}]) \tag{3.18}$$

The operating expenditures for solar panels and wind turbines are the only costs that don't depend on time. In fact, the fixed operation and maintenance costs or FO&M, which have been described in chapter 2, are expressed in €/kW/year. Therefore, they are multiplied by the installed electric power and cover the operational costs for one year.

- $C_{\text{Grid interaction}}$ [$\forall$ nd in decentral nodes, $\forall$ t in time steps] :

$$\sum_{nd} |\sum_{t} c_{\text{elec}}[\text{nd,t}] \cdot \text{Net exchange}[\text{nd,t}] \cdot \text{weight}[\text{t}]| \tag{3.19}$$

This part of the objective function focuses on the interaction between each company,i.e. decentral nodes, and the grid. A first assumption is that the grid is already established and fully operational. It is also the only interaction with an external player. In EXPRESSION 3.19, c_{elec}[nd,t] is the electricity price at each hour. As a reminder, the companies are distributed into three consumer profiles. Further, as the name suggests, Net exchange[nd,t] is a continuous variable referring to the purchases and injections of electricity to the grid. The variable is positive if energy is withdrawn from the grid and negative if it is injected into it.

Because companies are prosumers, the charging system has to include the potential injections coming from solar panels installed on their roofs. Therefore, the principle of net-metering is used to describe the interaction. This method basically means that the prosumer only pays the for the net electricity imported from the grid. In practice, a sum of all the loads and injections is effectuated over a period usually fixed at 1 year. However, the net price to be paid can not be negative, which explains why an absolute value appears in EXPRESSION 3.19. This approach enables to model efficiently the exchanges with the grid without caring about revenue prices, that are difficult to estimate on an hourly basis. Indeed, some articles presented in the literature review encountered issues at moments when revenues were higher than electricity prices. An overproduction would then happen at these moments in order to make a maximum of profits. This is impossible when using the net-metering method.

Note that the smallest values of c_{elec}[nd,t] have been rounded to zero in order to reduce as much as possible the range of coefficients in the objective function. Indeed, if the range is wide, numerical instabilities appear that may lead to very time-consuming computations or even make the model infeasible. The assistance of the solver Gurobi

Optimzation [50] suggests that the ratio of the largest to the lowest coefficient should be lower than 10^9. Having some high investment costs, it is necessary to make this rounding so that the limit is not crossed.

Numerically, the absolute value function is not linear, which is a problem when considering only linear functions and constraints. But, it has the property to be convex. In the optimisation domain, convexity enables to rewrite a non-linear function into a linear one by using some tricks. In this case, the absolute value is linearised as follows :

$$\sum_{nd} \cdot \text{bound[nd]} \tag{3.20}$$

$$\sum_{t} c_{\text{elec}}\text{[nd,t]} \cdot \text{Net exchange[nd,t]} \cdot \text{weight[t]} \leq \text{bound[nd]} \tag{3.21}$$

$$-\text{bound[nd]} \leq \sum_{t} c_{\text{elec}}\text{[nd,t]} \cdot \text{Net exchange[nd,t]} \cdot \text{weight[t]} \tag{3.22}$$

A new positive variable bound_{nd} is minimized and tightens the expression in the absolute value. Doing so, only linear functions and constraints are remaining after the reformulation.

- $C_{\text{Pumping power}}$ [∀ e in edges, ∀ t in time steps] :

$$\sum_{t} (c_{\text{elec}}\text{[t]} \cdot (\text{pump}_{\text{fraction}} \cdot (\sum_{e} \text{Heat inflow[e,t]}) - \text{Pump power[t]}) \cdot \text{weight[t]}) \tag{3.23}$$

In a district heating network, pumps are needed to put the water in motion and distribute heat to consumers. To do so, pumps require some electric power. The amount of energy is dependent on the heat flow entering each edge of the network. It is represented by the term : $\text{pump}_{\text{fraction}} \cdot (\sum_e \text{Heat inflow[e,t]})$. The coefficient $\text{pump}_{\text{fraction}}$ is set to 8.5% and makes the conversion between heat flows and required pumping power [19]. This term thus expresses the total amount of electricity needed to make the water flow in all the pipes.

In the next sections, it will be shown that the electricity produced on-site by centralised technologies, i.e. wind turbines or chp plants, is distributed to all consumers like in a micro-grid. Moreover, it also has the possibility to satisfy partly or totally the power consumption of pumps. It is modelled by the variable Pump power[t], which refers to the quantity of power dedicated to pumping needs. This variable is subtracted to the total required pumping demand as shown in Expression 3.23. The net pumping load is then multiplied by c_{elec}[t], which corresponds to the electricity price for large consumer profiles. Finally, the pumping power supplied by on-site productions can physically not be higher than the total required power. This is satisfied by adding the constraint below.

$$\text{Pump power[t]} \leq \text{pump}_{\text{fraction}} \cdot (\sum_{e} \text{Heat inflow[e,t]}) \tag{3.24}$$

Subsidies

The subsidy considered in this work concerns large installations[2] such as those at central nodes. The support is thus only available for biomass/biogas chp plants and

[2] At least 25 000€ of investments [49]

wind turbines. The reimbursement is calculated based on the additional investment costs to settle renewable technologies in comparison to conventional fossil-fueled plants. This can be written as follows :

$$25\% \cdot \sum_{n} \sum_{chp} (\mathrm{C}_{\text{Heat plants}}[\text{chp}] - (a_{\text{boiler}} \cdot (\mathrm{P}[\text{n,chp}] - \mathrm{P}_{\text{min}}[\text{n,chp}]) + b_{\text{boiler}} \cdot \delta[\text{n,chp}]) \tag{3.25}$$

$$25\% \cdot \sum_{n} ((c_{\text{invest}}[\text{wt}] - c_{\text{genset}}) \cdot (P_{\text{elec}}[\text{n,wt}] - P_{\text{elec,min}}[\text{n,wt}])) \tag{3.26}$$

For both formulations, the support is rated at 25% of the difference in prices, as mentioned in chapter 2. For chp plants, Expression 3.25 shows that the subtraction is taken between the cost of a chp heat plant detailed earlier and the cost for the same capacity if a natural gas boiler was considered. The same observation can be made for wind turbines, which are compared to diesel gensets in Expression 3.26.

3.3 Constraints

This section is organized in different categories that regroup the constraints according to their utility in the model.

3.3.1 Energy conservation

Heat energy balances

i) **Heat losses** [∀ e in edges, ∀ t in time steps] :

Expression 3.28 shows how heat losses are evaluated in the system. The coefficients $a_{\text{heat loss}}$ and $b_{\text{heat loss}}$ have been introduced in chapter 2. The factor 10^{-3} multiplies the equation because the heat loss parameters are expressed in W/m, while all constraints are in kW or kWh. Then, Expression 3.27 expresses the heat flow balance in a pipe. The heat inflow is limited by the capacity of the pipes, see Expression 3.29. In the case no pipe is built at a specific edge, the binary variable α[e]=0 and pipe_{cap}[e] is null too due to the previous Expression 3.13. This forces all heat flow variables to be equal to 0 and logically, no distribution is enabled when the decision variable α[e]=0.

$$\text{Heat inflow[e,t]} = \text{Heat outflow[e,t]} + \text{Heat losses[e,t]} \tag{3.27}$$

$$\text{Heat losses[e,t]} = 0.001 \cdot \text{Length[e]} \cdot (a_{\text{heat loss}} \cdot \text{pipe}_{\text{cap}}[\text{e}] + b_{\text{heat loss}} \cdot \alpha[\text{e}]) \tag{3.28}$$

$$\text{Heat inflow[e,t]} \leq \text{pipe}_{\text{cap}}[\text{e}] \tag{3.29}$$

ii) **Central nodes balance** [∀ nc in central nodes, ∀ t in time steps] :

The net amount of heat produced or received at central nodes is given by Expression 3.30. It corresponds to the sum of heat produced by all technologies available at a central node minus the proportion of energy that is stored in the thermal storage tank.

$$\dot{Q}_{\text{central}}[\text{nc,t}] = \sum_{te}(\text{power}[\text{nc,te,t}]) - \text{Storage}_{\text{injection}}[\text{nc,t}] \tag{3.30}$$

$$\dot{Q}_{\text{central}}[\text{nc,t}] = \sum_{e}(\text{Heat inflow}[\text{e,t}] \cdot \text{Connection}_{\text{in}}[\text{e,nc}] - \text{Heat outflow}[\text{e,t}] \cdot \text{Connection}_{\text{out}}[\text{e,nc}]) \tag{3.31}$$

Furthermore, the produced thermal power $\dot{Q}_{\text{central}}[\text{nc,t}]$ has to be delivered to the pipe network so that heat is distributed to consumers. The interaction with the district network is represented in Expression 3.31. $\text{Connection}_{\text{in}}[\text{e,nc}]$ is fixed in advance and it returns 1 if central node *nc* corresponds to the entry of edge e and 0 otherwise. Conversely, $\text{Connection}_{\text{out}}[\text{e,nc}]$ outputs 1 if a central node is at the end of an edge.

Doing so, an energy balance is effectuated between all the edges that are connected to a particular node. As Heat inflow[e,t] corresponds to the flow at the entry of an edge, it represents the stream exiting the node. Consequently, when $\dot{Q}_{\text{central}}[\text{nc,t}]$ is positive, heat is thus added to the district network, whereas if it is negative, heat from the district heating is stored in the thermal storage as no demands are assumed at central nodes.

iii) **Decentral nodes balance** [$\forall$ nd in decentral nodes, $\forall$ t in time steps] :

The heat loads at decentral nodes can be satisfied by two means. First, local production can be used and is represented by the variable power[nd,te,t]. Secondly, heat can originate from the district network, labelled $\dot{Q}_{\text{decentral}}[\text{nd,t}]$ in Expression 3.33.

$$\dot{Q}_{\text{decentral}}[\text{nd,t}] + \sum_{te}(\text{power}[\text{nd,te,t}]) = \text{Demand}[\text{nd,t}] \tag{3.32}$$

$$\dot{Q}_{\text{decentral}}[\text{nd,t}] = \sum_{e}(\text{Heat outflow}[\text{e,t}] \cdot \text{Connection}_{\text{out}}[\text{e,nd}] - \text{Heat inflow}[\text{e,t}] \cdot \text{Connection}_{\text{in}}[\text{e,nd}]) \tag{3.33}$$

Similarly to central nodes, an energy balance comprising the flows of the edges meeting at the node is established in Expression 3.33. However, the sign of $\dot{Q}_{\text{decentral}}[\text{nd,t}]$ has been inverted in this case. In fact, when it is positive (resp. negative), the prosumer consumes (resp. provides) heat from (resp. to) the network.

As mentioned previously, the substation is designed with respect to the highest peak load over the whole year. Therefore, the heating power that can be transferred through the heat exchanger is also limited by this maximum consumption. The following constraints make sure the interaction between a company and the district network can not exceed this limit. As a reminder, $\beta[\text{nd}]$ is the binary variable that decides whether or not a connection with the district network is made.

$$\dot{Q}_{\text{decentral}}[\text{nd,t}] \leq \beta[\text{nd}] \cdot Q_{\text{max}}[\text{nd}] \tag{3.34}$$

$$-\beta[\text{nd}] \cdot Q_{\text{max}}[\text{nd}] \leq \dot{Q}_{\text{decentral}}[\text{nd,t}] \tag{3.35}$$

Electric energy balances

i) **District scale** [∀ t in time steps] :

At each time step, there are two ways to produce electricity at a district scale. Both methods are shown in the right-hand side of Expression 3.36. It can be seen that the total power is composed of the electricity produced by all chp plants and wind turbines present on-site. Concerning chp plants, electricity is considered as a by-product. Indeed, chp plants have to be driven by heat demands in order to be efficient [12]. This is explained by the small electric efficiencies proper to chp technologies. The conversion from heat to electric power is enabled by the factor $\frac{\epsilon_{\text{elec}}[\text{chp}]}{\epsilon_{\text{heat}}[\text{chp}]}$, which is the ratio of the electric-to-heat efficiencies. The latter are assumed constant over the range of application, which is a good approximation when a minimum part load constraint has been added.

The other term in the right-hand side is the production from wind turbines. As explained in chapter 2, the hourly production is based on measured data from 2018. This is modelled by $\text{prod}_{\text{fraction}}[\text{wt,t}]$, which contains the fraction of installed capacity that is produced at each time step.

$$\sum_{nd}(\text{P}_{\text{central}}[\text{nd,t}]) + \text{Pump power}[\text{t}] = \sum_{nc}\sum_{chp}(\text{power}[\text{nc,chp,t}] \cdot \frac{\epsilon_{\text{elec}}[\text{chp}]}{\epsilon_{\text{heat}}[\text{chp}]}) + \sum_{nc}(\text{prod}_{\text{fraction}}[\text{wt,t}] \cdot \text{P}_{\text{elec}}[\text{nc,wt}]) \quad (3.36)$$

The left hand-side shows the potential use for this electric power. As already mentioned in Section 3.2, a part can be used to supply the energy demands of district pumps. The other possibility is to meet the needs of companies in case of production shortage by their PV panels. This is further detailed in the following section.

ii) **Building scale** [∀ nd in decentral nodes, ∀ t in time steps] :

Expression 3.37 represents the electric energy balance at a company of the industrial park. Most of the variables have already been introduced, such as Net exchange[nd,t], which describes the interaction with the grid. It can be positive or negative so that imports and exports are possible. Then, $\text{P}_{\text{central}}[\text{nd,t}]$ is a proportion of the electric power coming from large local plants and $\text{prod}_{\text{fraction}}[\text{pv,t}] \cdot \text{P}_{\text{elec}}[\text{nd,pv}]$ refers to the power production from the PV panels of the firm.

This power serves to satisfy the electric demands and potential supplementary loads from heat pumps. Implementing the heat pump requirements like this enables to take local production into account. This way, it could sometimes be free to run a heat pump when the irradiation is high. This synergy is not considered when using a pre-fixed hourly price.

$$\text{Net exchange}[\text{nd,t}] + \text{P}_{\text{central}}[\text{nd,t}] + \text{prod}_{\text{fraction}}[\text{pv,t}] \cdot \text{P}_{\text{elec}}[\text{nd,pv}] = \text{Demand}_{\text{elec}}[\text{nd,t}] + \sum_{hp}\frac{\text{power}[\text{nd,hp,t}]}{\text{cop}[\text{t}]} \quad (3.37)$$

3.3.2 Thermal storage

Implementation

The dynamic model of thermal storage can be viewed in Expression 3.38. The future level is dependent on the actual storage level and on heat loads/injections that occur at present time. Initial and end storage values have been fixed in Expressions 3.39 and 3.40. The coefficient $\mathrm{a}_{\mathrm{loss}}$ takes heat losses with the environment into account. The temperature inside the tank is assumed constant[3] and power losses are thus purely numerical [22]. This approximation enables to simplify the temperature control system and to focus on energy exchanges.

$$\mathrm{Storage}_{\mathrm{level}}[\mathrm{n,t+\Delta t}] = \mathrm{Storage}_{\mathrm{level}}[\mathrm{n,t}] \cdot (1 - a_{\mathrm{loss}}) - \mathrm{power}[\mathrm{n,sto,t}] + \mathrm{Storage}_{\mathrm{injection}}[\mathrm{n,t}] \tag{3.38}$$

$$\mathrm{Storage}_{\mathrm{level}}[\mathrm{n,0}] = 25\% \cdot P[\mathrm{n,sto}] \tag{3.39}$$

$$\mathrm{Storage}_{\mathrm{level}}[\mathrm{n,end}] = 25\% \cdot P[\mathrm{n,sto}] \tag{3.40}$$

Limitations

Expression 3.41 guarantees that the storage level will never exceed the total installed capacity. In addition, Expressions 3.42 and 3.43 constrain the maximum amount of power consumed or injected at a specific time due to technical limitations.

$$\mathrm{Storage}_{\mathrm{level}}[\mathrm{n,t}] \leq P[\mathrm{n,sto}] \tag{3.41}$$

$$\mathrm{power}[\mathrm{n,sto,t}] \leq 40\% \cdot P[\mathrm{n,sto}] \tag{3.42}$$

$$\mathrm{Storage}_{\mathrm{injection}}[\mathrm{n,t}] \leq 40\% \cdot P[\mathrm{n,sto}] \tag{3.43}$$

3.3.3 Network limitations

Decision variables

Expression 3.44 makes sure that a single direction is chosen for the flow of water. Indeed, each pipe is associated to one direction. The program has thus the choice between building a pipe in the *e* or *e'* direction but not both. Allowing to work with two pipes and thus a bi-directional heat flow at an edge would require to model the temperature dynamics along the pipes. This becomes intractable when the configuration of the network has to be designed in addition to the operation strategy. To summarize, when a pipe is built, the supply and return are considered, but the circulation of the heat transfer medium is unique.

$$\alpha[\mathrm{e}] + \alpha[\mathrm{e'}] \leq 1 \tag{3.44}$$

$$\beta[\mathrm{nd}] \leq \sum_{e} (\mathrm{Connection}_{\mathrm{out}}[\mathrm{e,nd}] \cdot \alpha[\mathrm{e}] + \mathrm{Connection}_{\mathrm{in}}[\mathrm{e,nd}] \cdot \alpha[\mathrm{e}]) \tag{3.45}$$

Then, Expression 3.45 concerns the construction of substations at consumers. It avoids the case in which a substation would be installed, while no edge termination

[3]The temperature asked by the district heating network.

is connected to a node. In fact, β[nd] is forced to zero if the sum of the potential connections over all edges is null.

Next, a few constraints about heat and electricity plants are represented. Expressions 3.46 and 3.47 are bounded by $\text{Tech}_{\text{accepted}}$ for heat plants and wind turbines respectively. $\text{Tech}_{\text{accepted}}$ is fixed in advance and takes binary values. If it is 0 at a node and for a specific technology, it is forbidden to build the latter at that location. Otherwise, it is permitted and the optimisation decides whether or not to install a technology. For instance, it has been disallowed to construct wind turbines at decentral nodes, where companies are located.

$$\delta[\text{n,te}] \leq \text{Tech}_{\text{accepted}}[\text{n,te}] \tag{3.46}$$

$$\gamma_{\text{wt}}[\text{n}] \leq \text{Tech}_{\text{accepted}}[\text{n,wt}] \tag{3.47}$$

$$\sum_{te}(\delta[\text{n,te}]) + \gamma_{\text{wt}}[\text{n}] \leq 1 \tag{3.48}$$

Lastly, Expression 3.48 allows only one technology per node. At central nodes, the choice is made between large heat plants and wind turbines. Concerning decentral nodes, the decision is made between smaller technologies like heat pumps or boilers. However, solar panels and thermal storage are not included in this equation and can thus be installed on top of that.

Space limitation

As already mentioned in chapter 2, engie impact provided some data about the pv potential for each company, which depends on the available area on their roofs. Therefore, the installed capacity is physically limited and this is taken into account by the following formulations. Similarly, the thermal storage tanks have been limited in volume. V_{needed} and A_{needed} are expressed in $\frac{m3}{kWh}$ and $\frac{m2}{kW_{\text{th}}}$ respectively.

$$\text{P}[\text{n,sto}] - \text{P}_{\text{min}}[\text{n,sto}] \leq \text{Tech}_{\text{accepted}}[\text{n,sto}] \cdot \frac{V_{\text{avail}}[\text{n}]}{V_{\text{needed}}} \tag{3.49}$$

$$P_{\text{elec}}[\text{n,pv}] - P_{\text{elec,min}}[\text{n,pv}] \leq \text{Tech}_{\text{accepted}}[\text{n,pv}] \cdot \frac{A_{\text{avail}}[\text{n}]}{A_{\text{needed}}} \tag{3.50}$$

CO_2 emissions

At the beginning of Section 3.2, it was detailed how the initial multiple-objective function was modified into a single-objective one. The main idea was to replace the CO_2 term in the minimization by a constraint with an upper bound. This is shown in Expression 3.51 below. The sum of the emissions over all technologies on-site and for all periods has to be lower than a fixed value. In practice, the code did run several times for different values of lim_{co_2} so that a Pareto curve could be obtained.

$$\sum_{n}\sum_{te}\sum_{t}(\text{CO}_2[\text{te}] \cdot \text{power}[\text{n,te,t}] \cdot \text{weight}[\text{t}]) \leq \text{lim}_{\text{co}_2} \tag{3.51}$$

Chapter 4

Simulations

In the literature review, the contributions of this work were highlighted. Among them, the inclusion of characteristics related to 4^{th} generation district heating. Besides, the various degrees of centralisation and the scale economies of technologies were also part of this master thesis. The context presented in the introduction emphasized the urgent decisions that have to be taken in order to respect the future environmental challenges. Therefore, this section aims at demonstrating the utility of the tool in decision-making situations, in which lots of schemes have to be investigated.

Three different scenarios will be studied corresponding to three supply and return temperatures of the district heating. TABLE 4.1 resumes the temperature levels and the associated potential technologies. In fact, all technologies can not produce heat at any working temperature. As already discussed in chapter 2, natural gas boilers and thermal storage are assumed to work at any range. Same for heat pumps, provided that the right COP values are used for the corresponding case. Then, biomass and biogas chp plants are only able to yield heat at high temperatures and are thus not considered at lower degrees. At last, some Stirling engine technologies can supply thermal energy at 70°C and are thus only included in the second simulation but not the others.

For each test case, a Pareto front will be drawn and the optimal energetic mix will be analysed. Moreover, the operating strategies will be specified. The Pareto curves represent the total costs over the whole project in function of the CO_2 emissions. This means that for each configuration of district energy system, the price and the related amount of emitted CO_2 are given. This enables to take weighted decisions that are beneficial for a smooth ecological transition. Indeed, instead of installing only renewable energy productions, that would maybe cost too much money, a more transient alternative including part of fossil-fueled plants could be envisaged.

Despite using supercomputers from the CÉCI clusters, the computing time is extremely long if a full year is investigated on an hourly basis. For this reason, representative weeks have been chosen per month and weights have been attributed to estimate the values for a whole year. The selected weeks contained the monthly peak loads so that the design didn't underestimate the real demands.

In the coming sections, the same approach has been used to describe the different scenarios. For each of them, the model computed an optimal layout for three different CO_2 bounds. One case prohibited any emission, another allowed large quantities

	90-60°C	70-40°C	50-20°C
Biomass chp	✓	✗	✗
Biogas chp	✓	✗	✗
Stirling engine	✗	✓	✗
NG boilers	✓	✓	✓
Heat pumps	✓	✓	✓
Thermal storage	✓	✓	✓

Table 4.1: The three scenarios with their corresponding accepted heating technologies.

of emitted CO_2 by relaxing the constraint. Lastly, a third limitation considered an amount of CO_2 half-way between the two extrema. These three limitations will later enable to draw the Pareto curve for each working temperature range.

Then, each scenario is analysed starting with a global view of the total installed capacities in the district. Afterwards, the focus will be put on a single company in order to observe the interactions during the year with the grid and the district network. Finally the DHN configuration for each greenhouse gas limit will be displayed and will include the direction of the heat flows.

4.1 Scenario 1 : High temperatures (90°-60°)

In these working conditions, the heat losses are the most impacting, but it is also the scenario in which the most technologies are available. As explained before, Figure 4.1 shows the chosen heat and power sources as well as the total installed capacities covering the whole site. When the emissions are unrestricted, all the heat production comes from large biomass chp plants at central nodes. Especially, gasification based biomass chp has been selected by the model instead of biomass combustion. The latter is better suited for higher power ranges and has a lower electric efficiency. Note that the biomass chp is expressed in terms of thermal power in the figure.

As the environmental constraints become increasingly restrictive, more and more heat pumps are developed at the expense of the gasification chp technology. Concerning renewable energies, the number of installed photovoltaics remain nearly constant in any case. This is explained by the physical limit of surfaces on the roofs. Moreover, it can be noticed that only one wind turbine of 2.2MW is established for high emissions, whereas two are installed in the other energetic mixes. The reason for this wind production expansion is twofold. First, the apparition of heat pumps at companies increase the electric load and the photovoltaics are limited by the available area. Secondly, by reducing the emissions, the capacity of gasification chp plants is diminished, which represents a considerable loss in power supply.

As it is difficult to present the whole operation of the district energy system, the attention will be put on a chosen firm for each scenario. In this case, FRIANDA SA

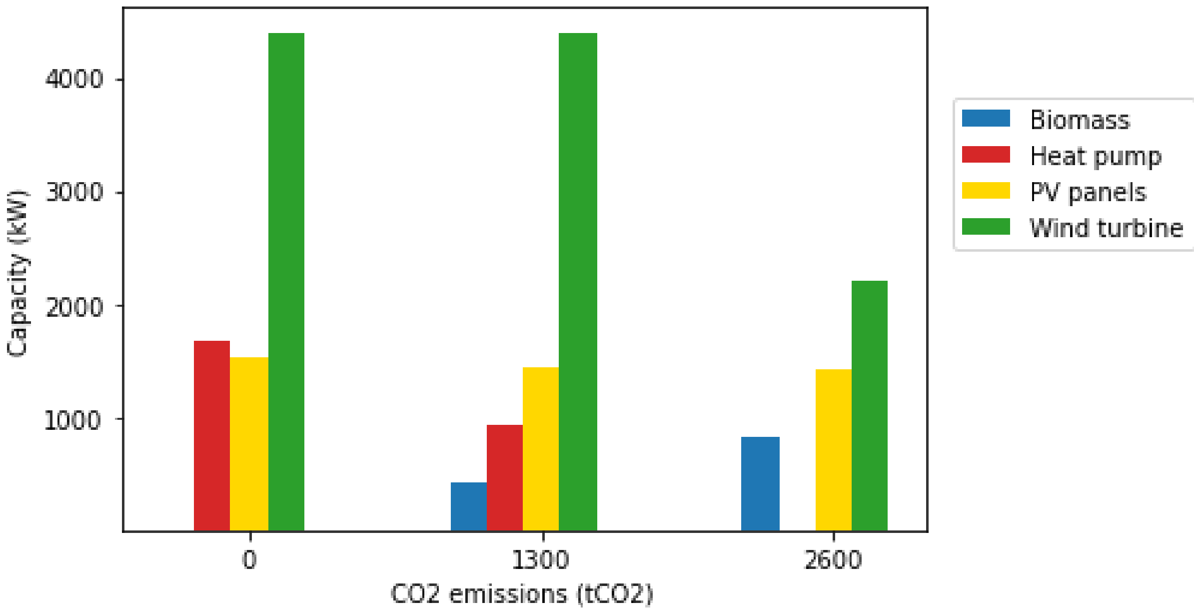

Figure 4.1: Total installed capacities for a heat supply temperature of 90°.

has been chosen to give an example of possible interactions on-site. Accordingly, FIGURE 4.2 contains the annual heat and electricity exchanges with the DHN and the grid respectively. Note that the bars are plotted relatively to each other, which means that no category is hided by another. The values in the bar graph may slightly overestimate the annual loads presented in chapter 2. Indeed, the computations were effectuated using representative weeks that included the monthly peak demand.

In the figure, heat and electricity interactions are shown together. This enables to make a first observation, which is that the company FRIANDA SA consumes more electric than thermal energy. The exchanges with the national grid are represented by 'Power export' and 'Power import'. The latter values are very similar due to the net-metering condition, which encourages auto-consumption. Then, the label 'Central power' refers to the proportion of electricity supplied by central installations such as biomass chp and wind turbines. As it corresponds to a local production, no net-metering is applied. In fact, the on-site electric production by centralised power plants is assumed to be distributed freely among the end-users. However, no interaction between the consumers is possible in the electricity sector.

At high emissions, it can be observed that the firm never exports heat. This means that no individual heat source is installed in that case and that the yearly heat load is entirely covered by centralised gasification chp plants. The situation is plotted in FIGURE 4.3(c). Indeed, it can be viewed that each decentralised node (blue) is connected to the DHN. Moreover, the heat flows all originate from a centralised node (red), at which a gasification chp is placed. The unconnected centralised nodes are either locations for wind turbines or unused at all.

Whenever the CO_2 bound is lowered, less fossil-fueled technologies are authorized, including central gasification chp. Therefore, small decentralised heat plants start to appear at companies. About FRIANDA SA, a heat pump is installed and the firm becomes a prosumer. Indeed, FIGURE 4.2 shows that it exports a part of its heat production.

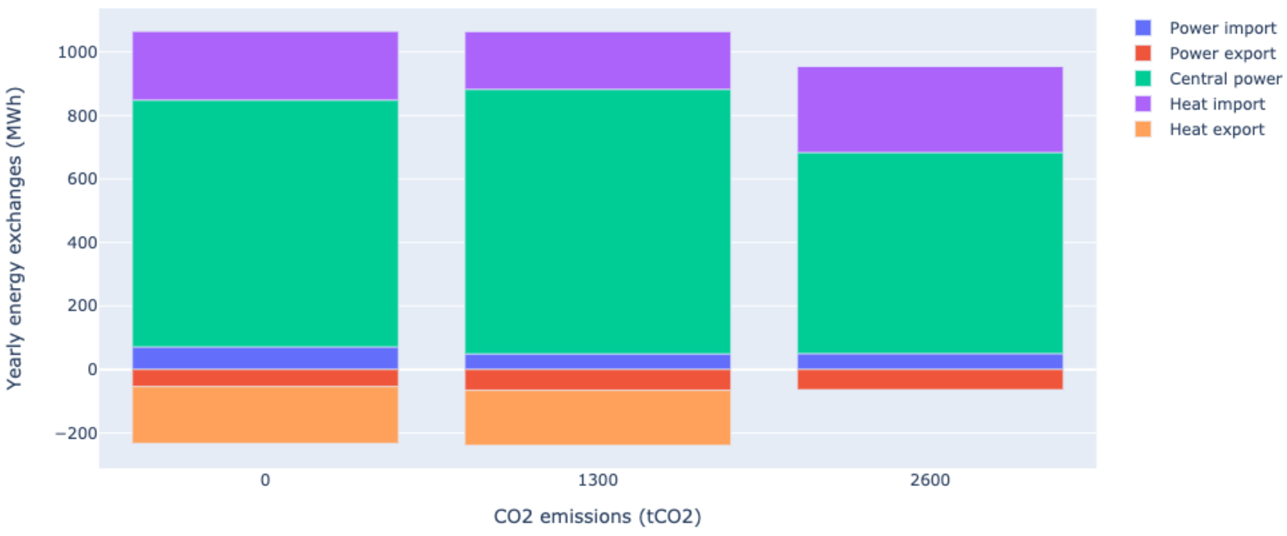

Figure 4.2: Annual energy exchanges for the company FRIANDA SA (SCENARIO 4.1).

FIGURE 4.3(b) shows the configuration at the district scale for 1300 tonnes of CO_2 emissions. A cluster of prosumers has been created in the upper-right corner, including FRIANDA SA. In addition, a smaller biomass gasification chp is still used to distribute heat to close companies in the left part of the figure. The remaining nodes are disconnected from the DHN and have to produce their thermal energy by themselves. It was not economically worth to associate them to the network as they are not huge consumers and they are also quite remote.

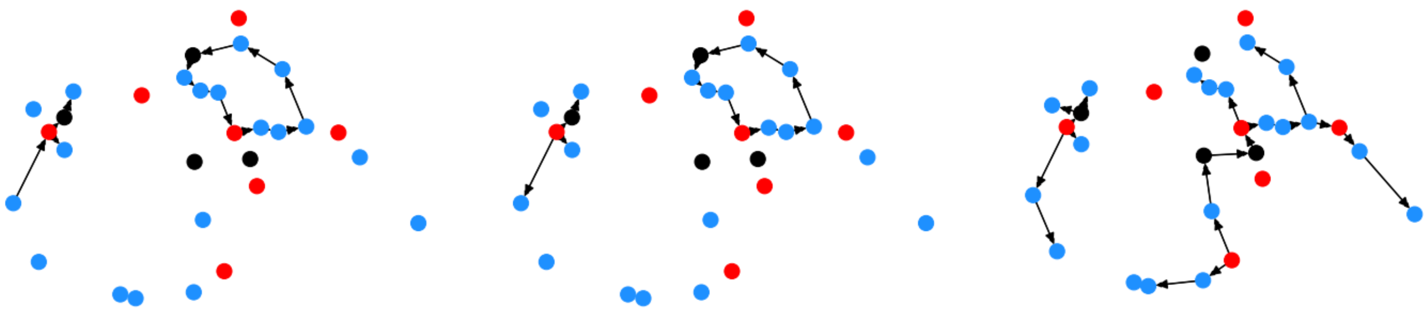

(a) 0 tCO_2 (b) 1300 tCO_2 (c) 2600 tCO_2

Figure 4.3: Representations of the heating networks for each CO_2 limitation.

At zero emissions of greenhouse gases, the behaviour of FRIANDA SA has not changed a lot. One particularity is that heat pumps have to be placed at every company in order to respect the environmental constraint. Therefore, a little less power is available from 'Central power' and more imports from the grid are required to meet the high electrical demands in this situation. The last case is drawn in FIGURE 4.3(a).

Finally, the capacities of thermal storage for the three examples above are detailed in TABLE 4.2. It can be observed that lots of storage means are employed when the

DHN is the most expanded.

	0 tCO_2	1300 tCO_2	2600 tCO_2
Storage capacity (MWh)	12.61	13.41	21.28

Table 4.2: Thermal storage for each CO_2 limit at a supply temperature of 90°.

4.2 Scenario 2 : Mid temperatures (70°-40°)

As a reminder, the only available biomass technology at this temperature level is the Stirling engine. As previously, Figure 4.4 shows the resulting mix of technologies that has been selected in the optimal design. It can be seen that for unrestricted emissions, the quantity of CO_2 is higher than in the preceding scenario. This is explained by the presence of natural gas boilers, which are the highest CO_2 emitters of all technologies.

As already observed, the fossil-fueled heating sources decrease with decreasing greenhouse emissions and disappear at zero. However, a particularity arises in this context. Indeed, heat pumps and wind turbines are already predominantly included in the district configuration for large amounts of CO_2. This is due to the poor utility of the Stirling engine technology regarding electric power supply. In fact, the electric efficiency of this chp plant is the lowest of all biomass technologies. For this reason, Stirling engines have less impact than gasification biomass and it is reflected below. This observation is proper to this case study and it may be different for other districts with less electric loads.

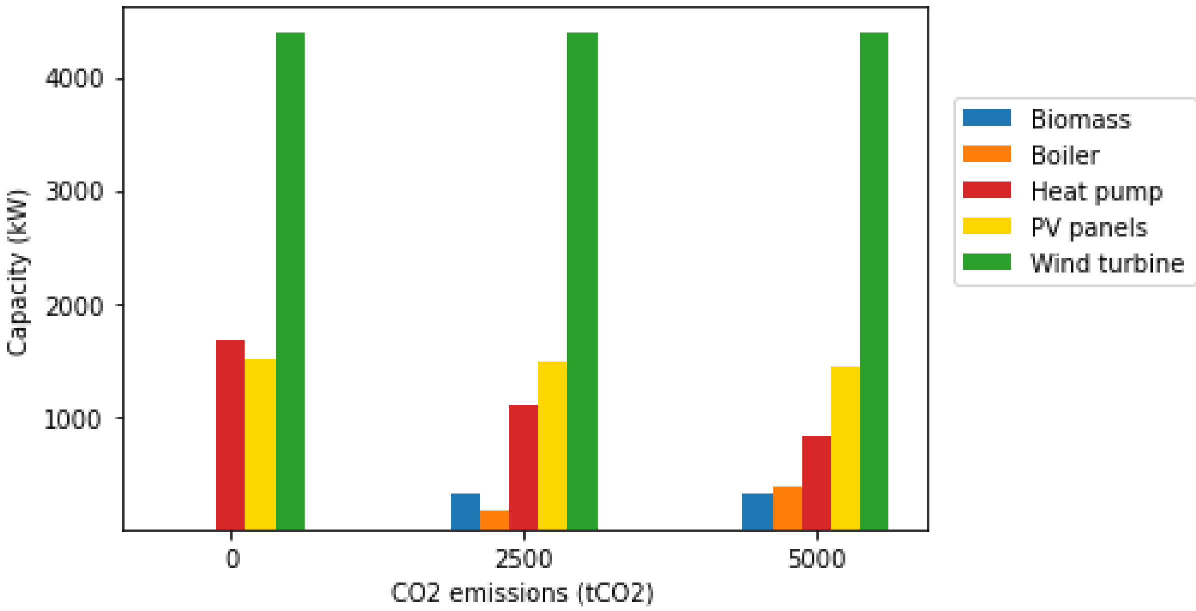

Figure 4.4: Total installed capacities for a heat supply temperature of 70°.

The same way it has been done before for FRIANDA SA, a detailed analysis of the energy transfers for a specific company will be effectuated. The selected firm is CON-

SOLIDATED PRECISION PRODUCTS and is the leftmost point in the representations of the DHN in FIGURE 4.6. This corporation has been chosen because the behaviour changes with the different CO_2 levels. Note that for the majority of the companies, the interactions didn't change that much as reflected by the three network layouts, which are very similar. Indeed, no additional connections nor synergies appear when the quantity of emissions is varied. Individual fossil-fueled heat plants are generally just replaced by heat pumps when the allowed emitted CO_2 is lowered.

Concerning CONSOLIDATED PRECISION PRODUCTS, it can be viewed in FIGURE 4.5 that the firm imports all its heat consumption for both greenhouse gas emitting cases. This thermal energy is provided by the central Stirling engine situated at the closest central node and it is distributed by the DHN. Then, for the carbon-free layout, the same network linking the companies remains but part of the heat flows have changed their direction. This is represented in the left side of FIGURE 4.6(c), in which CONSOLIDATED PRECISION PRODUCTS becomes a prosumer and provides heat to the two other connected firms.

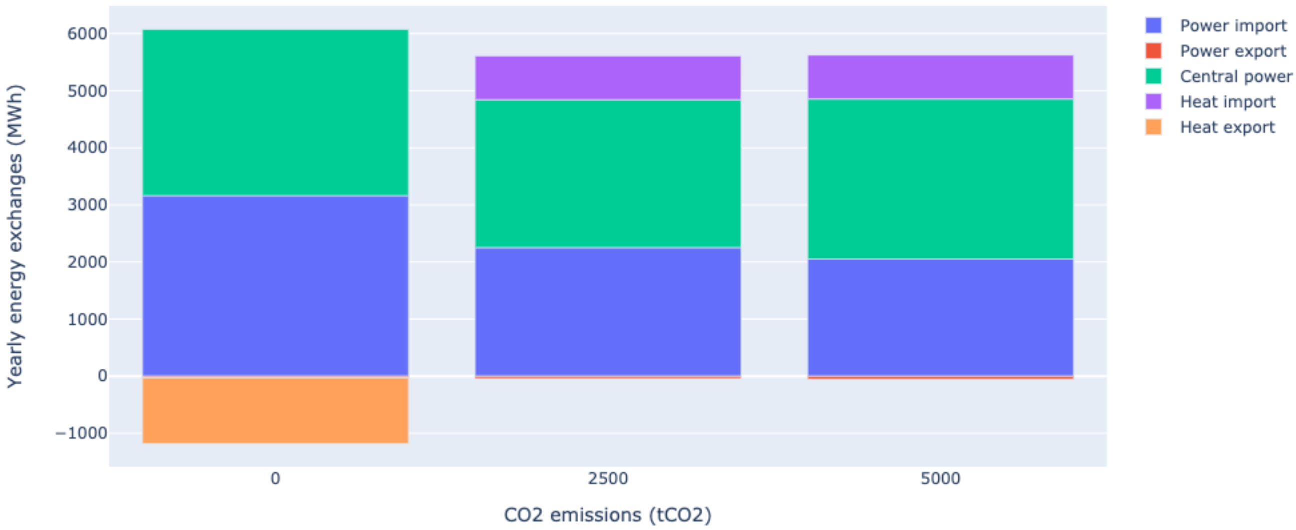

Figure 4.5: Annual energy exchanges for the company CONSOLIDATED PRECISION PRODUCTS (SCENARIO 4.2).

This role shift can be observed in FIGURE 4.5. In fact, when greenhouse gases are avoided, a large heat pump is installed at the company. The latter is thus self-sufficient and produces its own heat. Moreover, it exports also part of its production to supply the other companies linked to it. This behaviour requires additional amounts of power, which is also represented in the energy exchanges bar graph.

Finally, the thermal storage capacities are given for each situation in TABLE 4.3. The values are really close to each other because the three configurations are nearly equivalent.

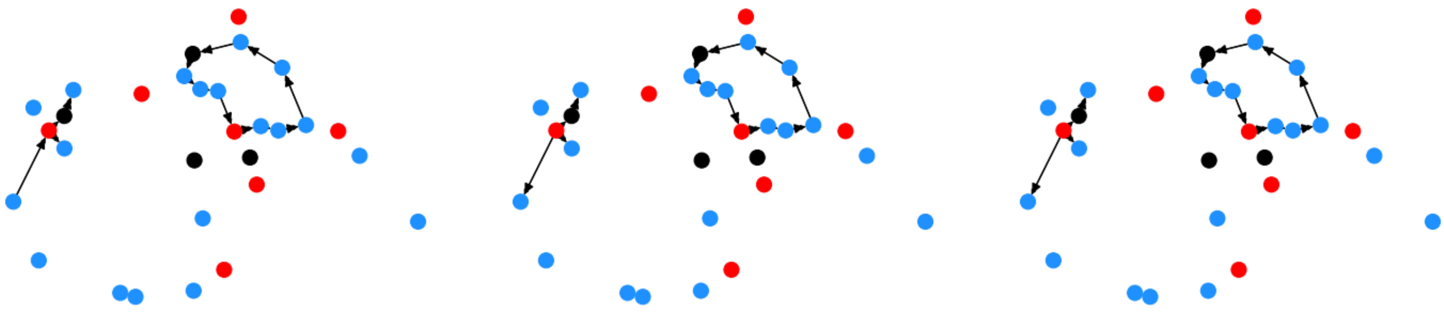

(a) 0 tCO_2 (b) 2500 tCO_2 (c) 5000 tCO_2

Figure 4.6: Representations of the heating networks for each CO_2 limitation.

	0 tCO_2	2500 tCO_2	5000 tCO_2
Storage capacity (MWh)	11.57	11.97	11.95

Table 4.3: Thermal storage for each CO_2 limit at a supply temperature of 70°.

4.3 Scenario 3 : Low temperatures (50°-20°)

At low-temperatures, the heat losses are the lowest and the COP values are much more interesting. Consequently, FIGURE 4.7 shows that a large proportion of heat pumps is already installed at high emissions of CO_2. The amount of emitted gas is thus also quite low in this scenario. However, natural gas boilers are still selected in the optimal design due to their low investment costs. Those are essentially installed at companies that are not connected to the DHN. As expected, only heat pumps remain when CO_2 emissions are prohibited.

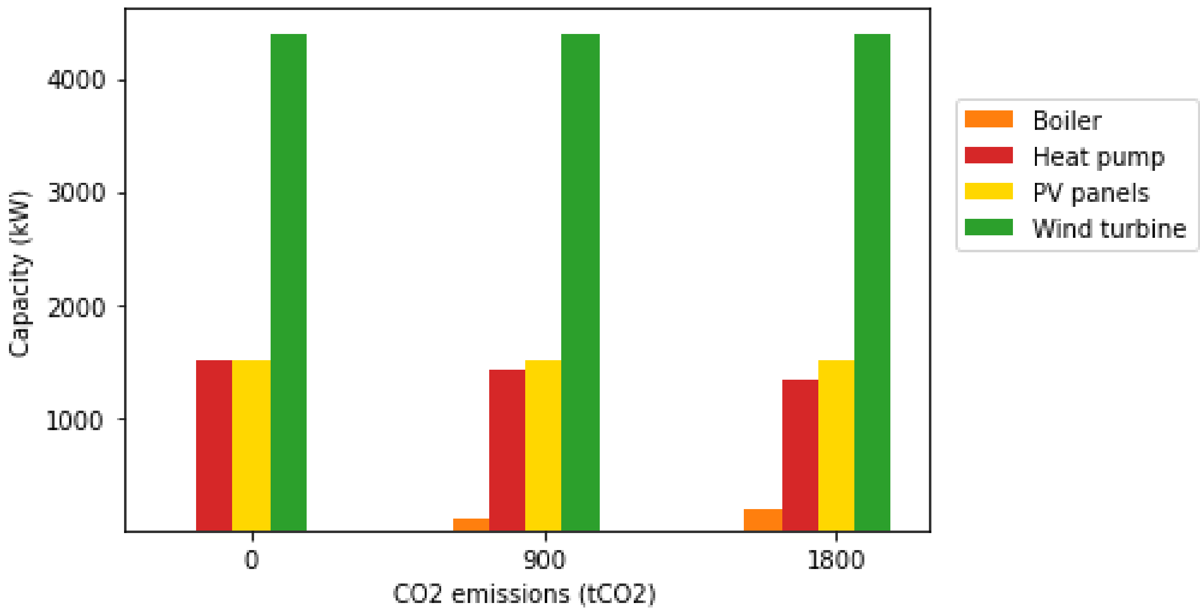

Figure 4.7: Total installed capacities for a heat supply temperature of 50°.

The company that will be studied in this case is PASTIFICIO DELLA MAMA. It is situated in the upper-left corner of the district layout. The exact location corresponds to node 9 and can be retrieved from FIGURE 2.1(a). FIGURE 4.8 resumes the different operating situations for the three environmental constraints. It can be viewed that PASTIFICIO DELLA MAMA never exports heat energy. Furthermore, the firm is not even connected to the district heating network when emissions are allowed, meaning that an individual heat source is thus installed. The node is effectively isolated in FIGURES 4.9(b) and 4.9(c).

In the carbon-free situation, a connection is established as can be seen in FIGURE 4.9(a). The company therefore starts to import a certain amount of heat per year. A heat pump is still needed to be installed at PASTIFICIO DELLA MAMA but the capacity has been reduced. Hence, the electric load is also decreased, which is observable in the left bar of FIGURE 4.8.

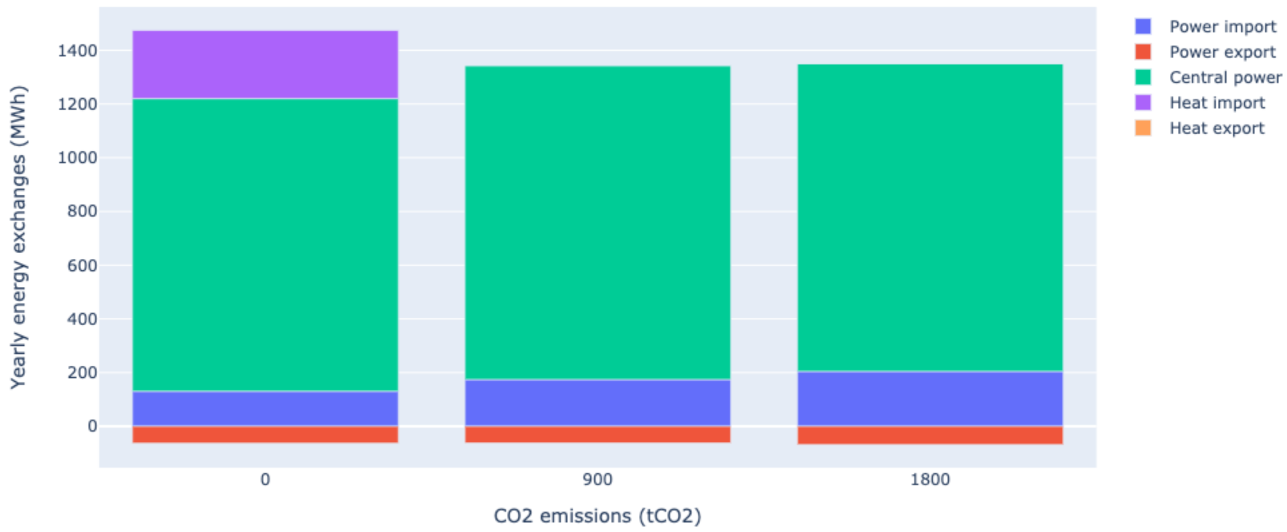

Figure 4.8: Annual energy exchanges for the company PASTIFICIO DELLA MAMA (SCENARIO 4.3).

At the district scale, the configurations of FIGURE 4.9 are not so different and companies once more keep more or less the same interactions. Some exceptions still happen such as the case of PASTIFICIO DELLA MAMA. This means that economically, it is not beneficial to create new interconnections, but it is preferred to replace natural gas boilers by heat pumps to reduce greenhouse gas emissions. This will have a particular impact on the Pareto curve, which will be explained in the next section.

Finally, the capacity of storage tanks is shown in TABLE 4.4. At 0 tonnes of CO_2, the amount of storage is similar to the previous scenario at 70° of supply temperature. For both other cases, the capacity is even lower because less connections are built.

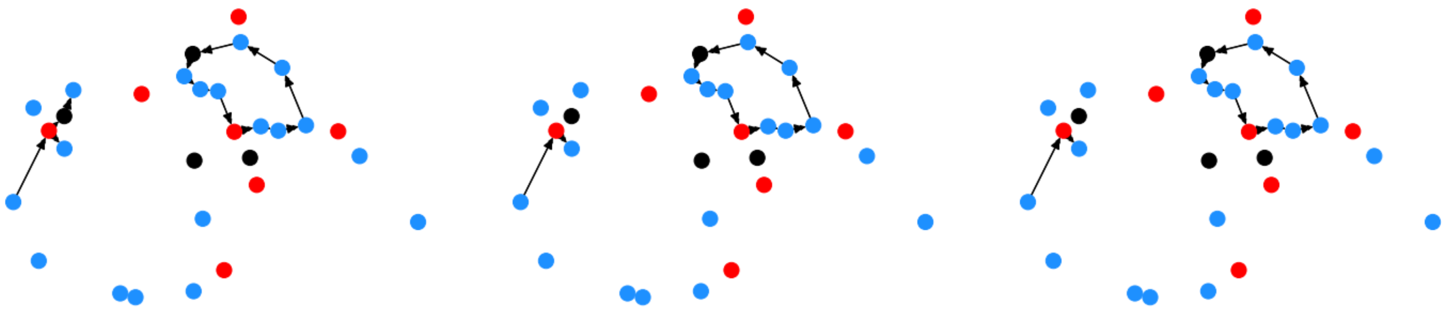

(a) 0 tCO_2 (b) 900 tCO_2 (c) 1800 tCO_2

Figure 4.9: Representations of the heating networks for each CO_2 limitation.

	0 tCO_2	900 tCO_2	1800 tCO_2
Storage capacity (MWh)	11.4	9.17	9.4

Table 4.4: Thermal storage for each CO_2 limit at a supply temperature of 50°.

4.4 Pareto curves

The Pareto fronts have been constructed by using information corresponding to every case discussed above. The latter are represented by dots for each temperature level in Figure 4.10.

First, the curve representing temperatures of 90°-60° will be analysed. It can be seen that, if gasification biomass is allowed to be used with respect to emission constraints, the overall costs can be drastically decreased. This is due to the excellent chp efficiencies at that temperature. Note that when gasification chp was fully used, the DHN included the most connections of any considered case. The combination of high efficiencies and large district networks explains the low costs that can be attained. In the carbon-free situation, no chp can be installed and the costs are similar to temperature levels of 70°-40°. They are even worse because heat losses are more important at higher working temperatures.

Concerning both 70° and 50° supply temperatures, the curves are much more flat. The reason for such a behaviour has been partly explained in the preceding sections. Indeed, it has been discussed that for these two temperature levels, the global trend following a decrease in the emissions was to substitute fossil-fueled heat technologies by heat pumps. No major changes in the network layout nor any impact of efficiencies was observed. Therefore, for both cases, the variation in overall costs only depends on investment and operating costs. As a result, because fossil-fueled heat plants have low investment and operating costs compared to heat pumps, the overall costs are lower when they are used in the energetic mix. Note that the costs for wind turbines and PV panels are included in the total costs and are significant. It can thus be assumed that if the project duration is increased, the ratio of renewable costs in the total costs would decrease and the carbon-free energetic mix could become the best economic option too.

To end with, the most important information retrieved from this model is resumed in the Pareto curves. In fact, they enable to have a visual support of all the plans that can be envisaged by decision-makers. The most interesting results for a real project would be to consider the lower bounds of all the curves. Indeed, if really low emissions are the main concern of a project, the DHN at 50°-20° temperatures is the best suited as it has the lowest overall costs. The reason is that heat losses are low and COP values for heat pumps are boosted in these ranges.

Then, if a certain amount of greenhouse gas is permitted, a district heating network at 90°-60° has to be envisaged. Indeed, overall costs are much lower as they benefit from the favourable chp efficiencies. In any case, building a DHN at a supply temperature of 70° seems not to be a profitable option. At these mid ranges, the DHN does not have the advantages of lower temperatures, which are low heat losses and efficient COP values. In addition, it neither has the pros of higher temperatures, which are high operating efficiencies.

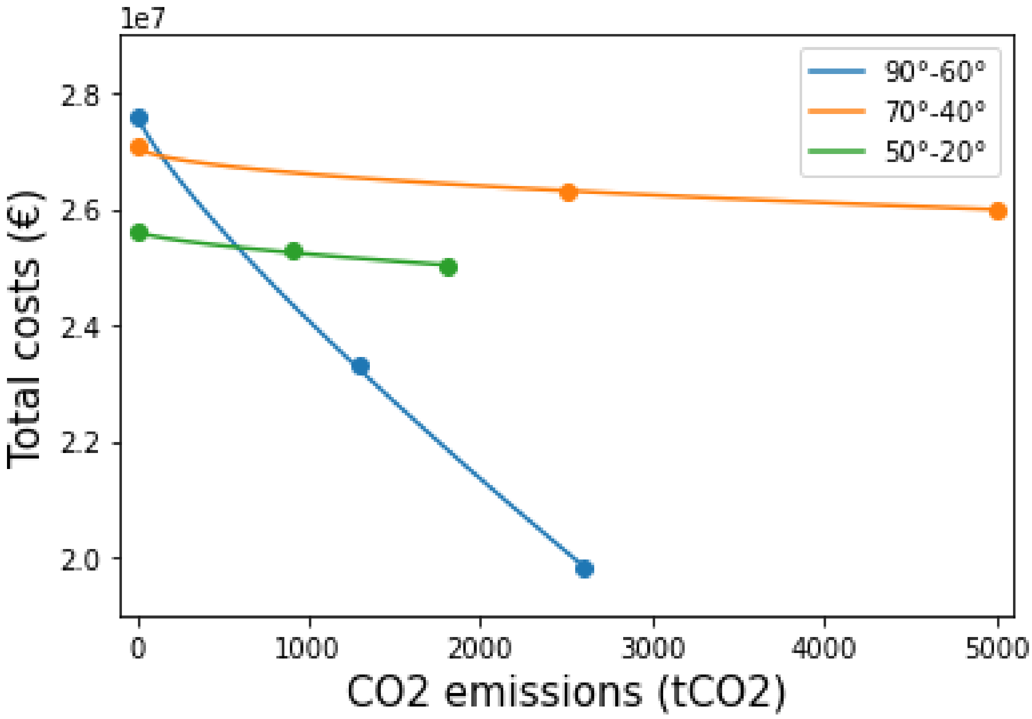

Figure 4.10: Pareto curves for all scenarios.

Chapter 5

Conclusion

In this work, a tool has been presented to evaluate the possibilities of adopting a district heating network coupled with a renewable energy system in a particular area. This study is in line with recent EU reports claiming that Belgium had to improve its environmental challenges. Moreover, the introduction brought to the fore the importance of local energy communities in the ecologic transition.

The case study that has been considered is the industrial park "Les Hauts-Sarts" located in Liège. A mixed-integer linear program is used to assess the optimal layout and operation strategy of a fourth-generation DHN. This family of programs has been chosen to obtain a robust model, while still guaranteeing a unique optimal solution. Both features are necessary to build a flexible program, which can be applied to any project.

The inputs of the model have been detailed in chapter 2. Both heat and power loads have been modeled on an hourly basis for each consumer. In addition, a wide selection of renewable and non-renewable technologies was investigated so that every potential synergy could be optimised. Linear regressions have been computed to handle non-linear functions. They were either used in piece-wise functions to approximate the costs of technologies or simply to linearise physical phenomena such as heat losses.

After, the mathematical equations composing the numerical program were expressed. In particular, each term from the objective function has been comprehensively described. Furthermore, the ϵ-constraint approach that has been used to obtain a single-objective function has been explained in chapter 3.

From then, three scenarios were established for three different supply temperatures. An optimal layout of the energy system was computed for various bounds of the ϵ-constraint. This is similar to study the optimal configuration as a function of the CO_2 limitation. These simulations enable to build the Pareto fronts for each scenario. Such curves give the total costs over the project duration for each greenhouse gas emission. This may guide the project executives to take decisions depending on their motivations, whether it is more economical or environmental.

The results obtained for the industrial park can be resumed as follows. If the focus is put on minimizing the emissions, low-temperature DHN (50°-20°) is the most economically interesting option. This is due to the low heat losses and the high COP values. In terms of operation, the district heating is primarily fed by heat pumps located at companies. The latter ones are either connected to the network and operate as prosumers. Or, the end-users are isolated and self-sufficient regarding their heat consumption. To support the additional electric loads from heat pumps, PV panels are largely installed on the roofs and two wind turbines are also added to the energetic mix.

If the focus is put on minimizing the overall costs, higher temperature ranges (90°-60°) are better suited. This can be explained by the fact that the gasification chp technology can deliver heat at this temperature and work at high efficiencies. In this situation, almost all companies are linked to the DHN. This means that most of the heat demands are met by large centralised chp plants and virtually no individual heat source is installed. Less renewable energies are also required as chp installations already provide part of the electricity to the community.

In future work, the integration of energy storage (such as batteries) may be interesting to study their influence on power exports and imports of companies. Other technologies such as fuel cells may also be included in the model, but will probably increase the computation time of the program. Then, instead of investing money only in technologies, investments in building retrofitting could also be considered. Finally, economic parameters like inflation could be introduced to better approximate future costs.

Appendix A

"Les Hauts-Sarts"

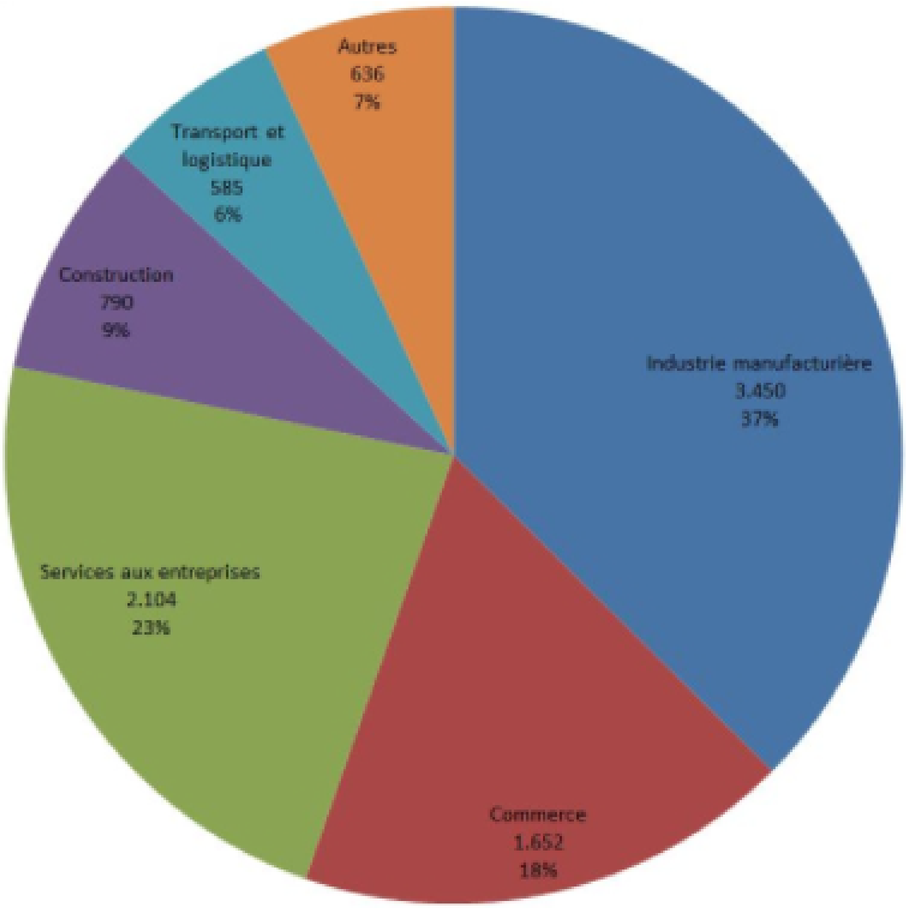

Figure A.1: Proportions regarding the business sectors of the industrial park [25].

Figure A.2: Map representing the 3 zones of the economic park [25].

Appendix B

Operational information about heating technologies

Characteristic	NG boiler small&mid	NG boiler large	Gasification chp	Combustion chp	Stirling Engine	Heat pump
Operational cost (€/kWh_{th})	0.05	0.04	0.029	0.029	0.031	/
Required area (m^2/kW_{th})	0.005	0.005	0.013	0.013	0.013	0.02
CO_2 emissions (kg of CO_2/kWh_{th})	0.2	0.2	0.025	0.058	0.025	0

Table B.1: Operational costs, required areas and CO_2 emissions for the different heating technologies [32, 33, 51–53].

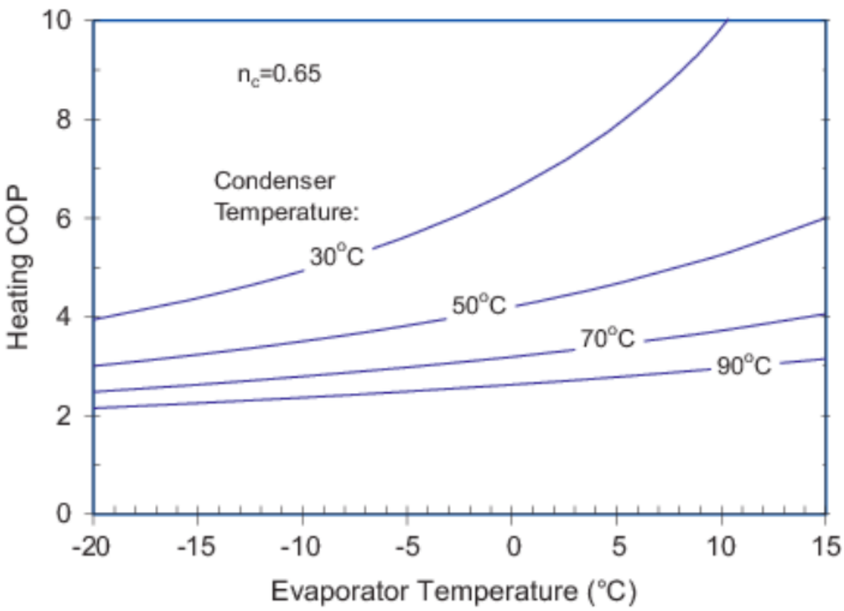

Figure B.1: Evolution of the COP for different condenser temperatures [54].

Appendix C

Information about electricity technologies and prices

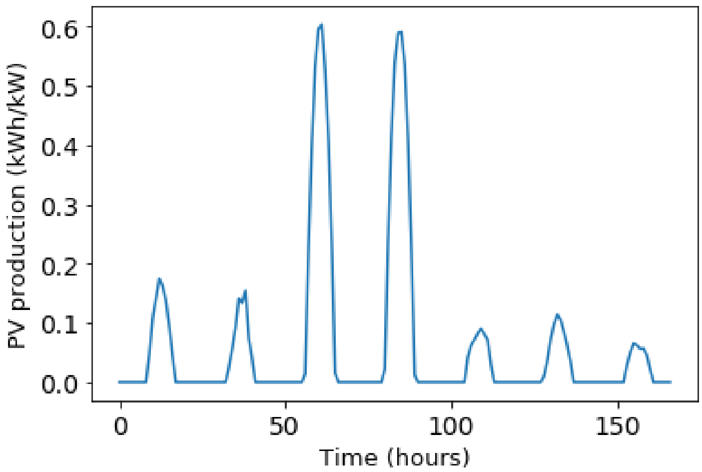

(a) Production for the week starting on Monday 12/02/2018

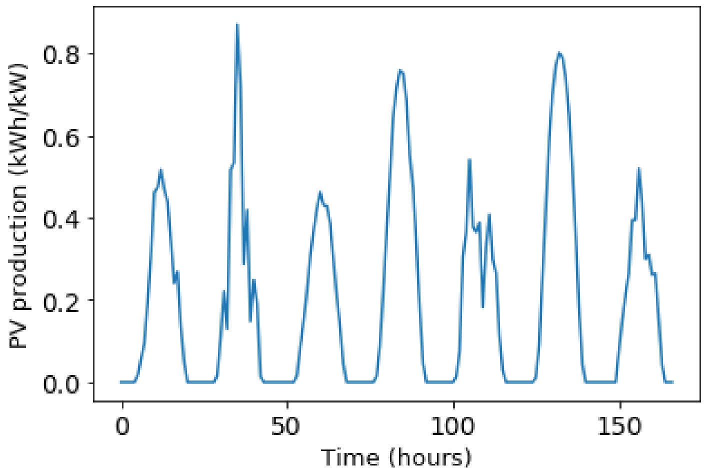

(b) Production for the week starting on Monday 16/07/2018

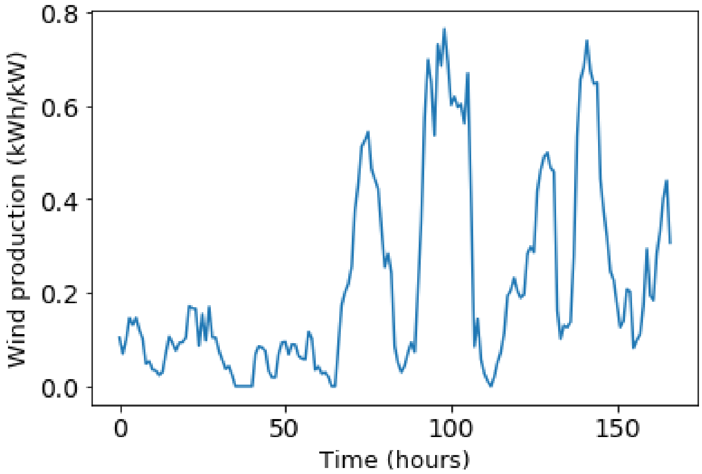

(c) Production for the week starting on Monday 12/02/2018

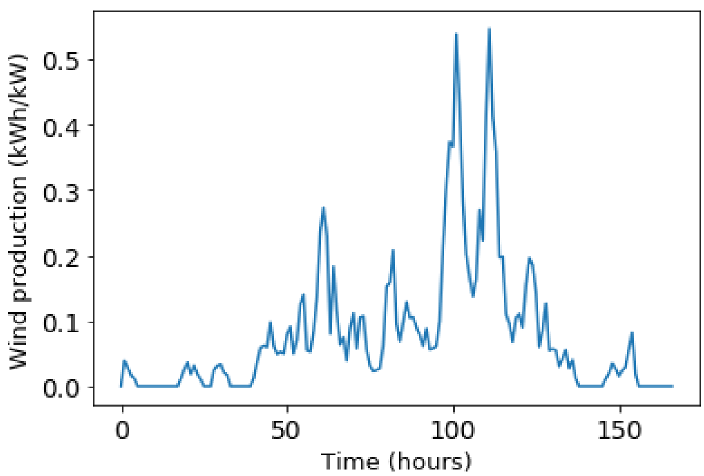

(d) Production for the week starting on Monday 16/07/2018

Figure C.1: Weekly power production from photovoltaics and wind turbines.

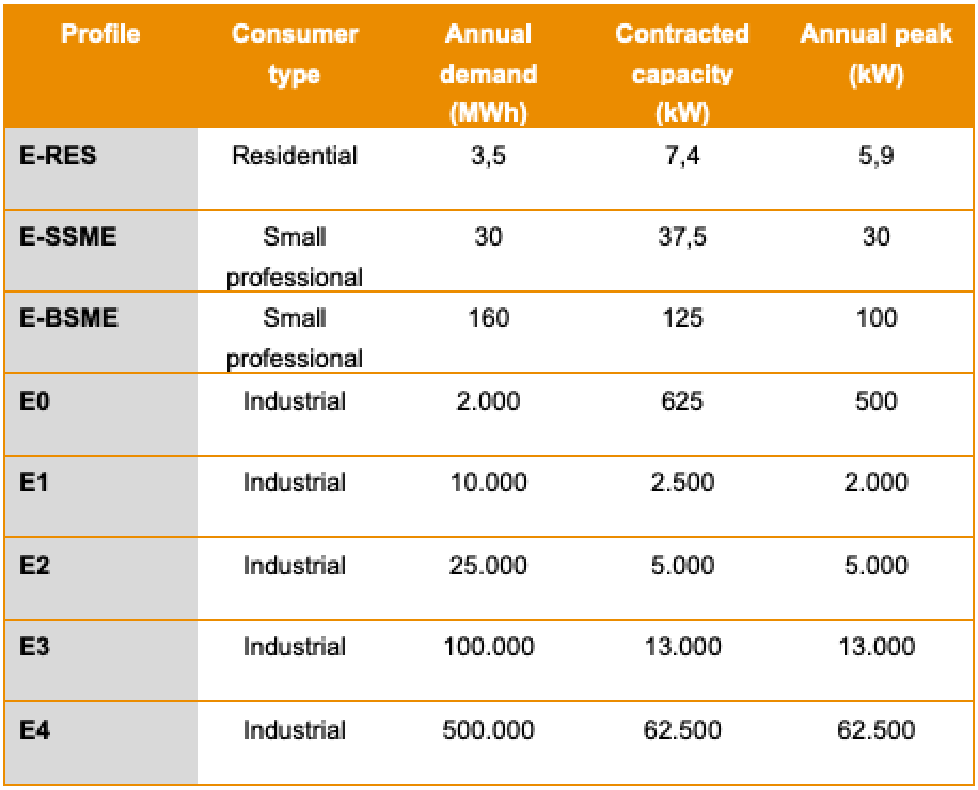

Profile	Consumer type	Annual demand (MWh)	Contracted capacity (kW)	Annual peak (kW)
E-RES	Residential	3,5	7,4	5,9
E-SSME	Small professional	30	37,5	30
E-BSME	Small professional	160	125	100
E0	Industrial	2.000	625	500
E1	Industrial	10.000	2.500	2.000
E2	Industrial	25.000	5.000	5.000
E3	Industrial	100.000	13.000	13.000
E4	Industrial	500.000	62.500	62.500

Figure C.2: Different electric consumer profiles established in [46].

Component	small professional	mid professional	large industrial
Commodity (%)	30.2	36	42.5
Network (%)	36.1	36.1	25.1
Other costs (%)	33.7	27.9	32.4

Table C.1: Proportions of each component in the electricity bill for different size of businesses [46].

Appendix D

Pipe costs and heat losses

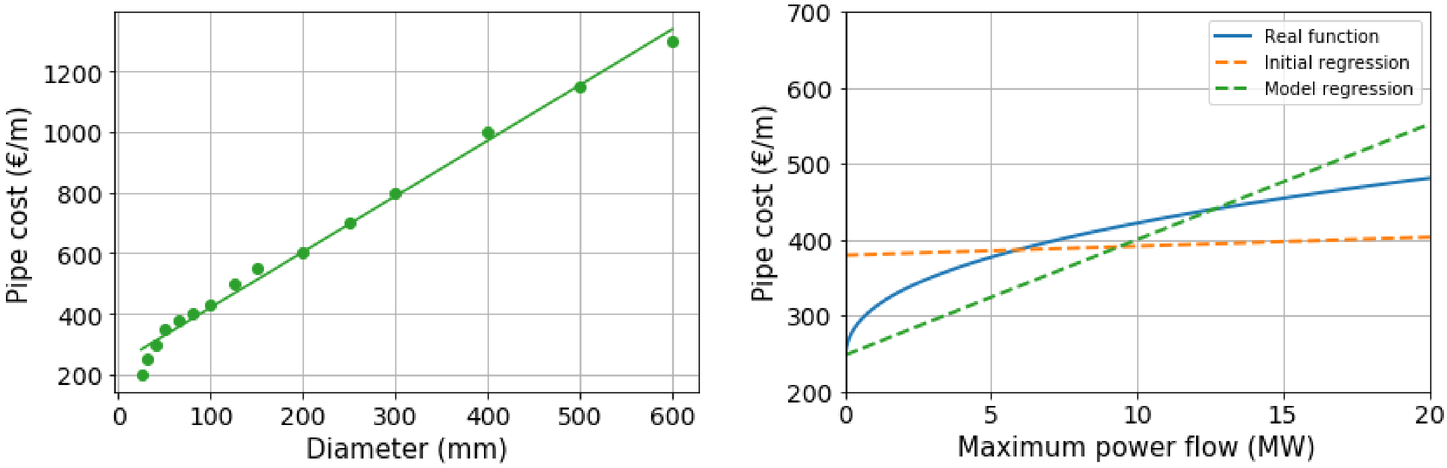

(a) Regression based on price data depending on diameters

(b) Linear regression of the non-linear pipe cost function

Figure D.1: Regressions that are used to obtain a linear function for pipe costs.

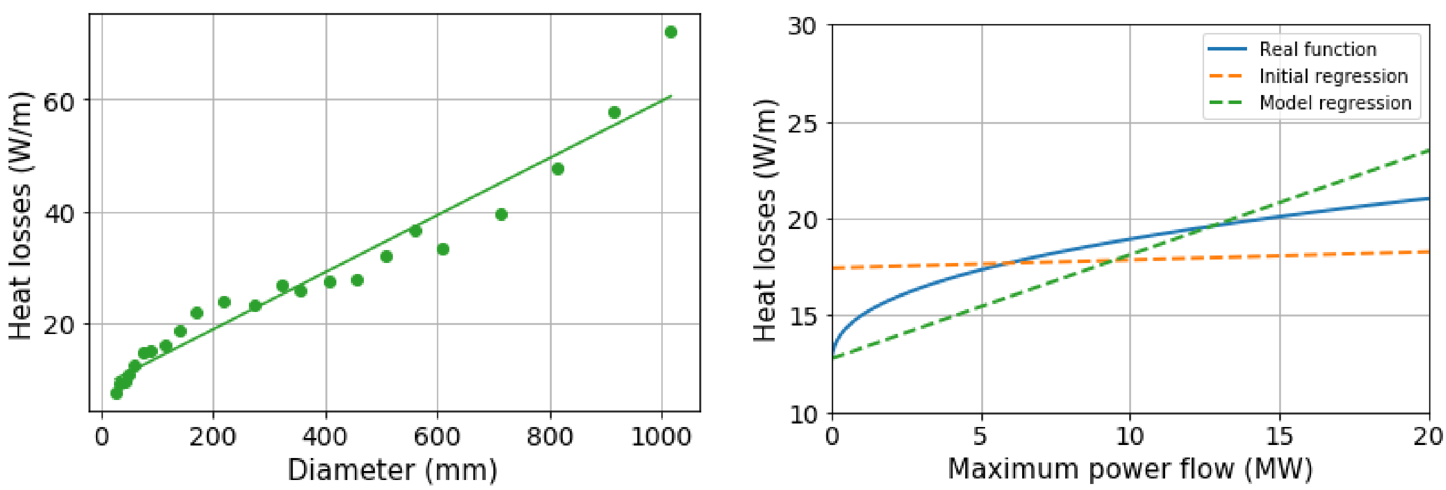

(a) Regression based on calculated points

(b) Linear regression of the heat loss function for a supply temperature of 90°C

Figure D.2: Regressions that are used to obtain a linear function for heat losses.

Bibliography

[1] United Nations. Paris agreement. https://unfccc.int/fr/processus-et-reunions/l-accord-de-paris/l-accord-de-paris, Consulted on 05/05/2021.

[2] European Union. Climate strategies targets. https://ec.europa.eu/clima/policies/strategies/2050_en, Consulted on 05/05/2021.

[3] Service Public Fédéral. Plan national Énergie-climat 2021-2030. https://climat.be/politique-climatique/belge/nationale/plan-national-energie-climat-2021-2030, Consulted on 06/05/2021.

[4] Energyprice. Energy mix in belgium: where does our electricity come from? https://www.energyprice.be/blog/energy-mix-belgium/, Consulted on 08/05/2021.

[5] Service Public Fédéral. La commission européenne évalue le plan national énergie-climat 2021-2030. https://climat.be/actualites/2020/la-commission-europeenne-evalue-le-plan-national-energie-climat-2021-2030, Consulted on 06/05/2021.

[6] David Connolly, Brian Vad Mathiesen, Poul Alberg Østergaard, Bernd Möller, Steffen Nielsen, Henrik Lund, Daniel Trier, Urban Persson, Daniel Nilsson, and Sven Werner. *Heat Roadmap Europe 1: First Pre-Study for the EU27*. May 2012.

[7] D. Connolly, H. Lund, B.V. Mathiesen, S. Werner, B. Möller, U. Persson, T. Boermans, D. Trier, P.A. Østergaard, and S. Nielsen. Heat roadmap europe: Combining district heating with heat savings to decarbonise the eu energy system. *Energy Policy*, 65:475–489, 2014.

[8] Danish Energy Agency. Technology data for individual heating plants. https://ens.dk/sites/ens.dk/files/Analyser/technology_data_catalogue_for_individual_heating_installations.pdf, Consulted on 21/05/2021.

[9] Henrik Lund, Sven Werner, Robin Wiltshire, Svend Svendsen, Jan Eric Thorsen, Frede Hvelplund, and Brian Vad Mathiesen. 4th generation district heating (4gdh): Integrating smart thermal grids into future sustainable energy systems. *Energy*, 68:1–11, 2014.

[10] Ministère de la transition écologique. Réseaux de chaleur. https://www.ecologie.gouv.fr/reseaux-chaleur#:~:text=Il%20est%20pr%C3%A9sent%20essentiellement%20pour,(r%C3%A9seau%20de%20la%20CPCU)., Consulted on 07/05/2021.

[11] European commission. Energy performance of buildings directive. https://ec.europa.eu/energy/topics/energy-efficiency/energy-efficient-buildings/energy-performance-buildings-directive_en#:~:text=Buildings%20are%20responsible%20for%20approximately,of%20the%20greenhouse%20gas%20emissions.&text=Renovation%20of%20existing%20buildings%20can,CO2%20emissions%20by%20about%205%25., Consulted on 07/05/2021.

[12] Jay Hennessy, Hailong Li, Fredrik Wallin, and Eva Thorin. Towards smart thermal grids: Techno-economic feasibility of commercial heat-to-power technologies for district heating. *Applied Energy*, 228:766–776, 2018.

[13] Euroheat Power. District energy explained. https://www.euroheat.org/knowledge-hub/district-energy-explained/, Consulted on 07/05/2021.

[14] T. Mertz, S. Serra, A. Henon, and J.M. Reneaume. A minlp optimization of the configuration and the design of a district heating network: study case on an existing site. *Energy Procedia*, 116:236–248, 2017. 15th International Symposium on District Heating and Cooling, DHC15-2016, 4-7 September 2016, Seoul, South Korea.

[15] Na Deng, Rongchang Cai, Yuan Gao, Zhihua Zhou, Guansong He, Dongyi Liu, and Awen Zhang. A MINLP model of optimal scheduling for a district heating and cooling system: A case study of an energy station in Tianjin. *Energy*, 141(C):1750–1763, 2017.

[16] Richard Krug, Volker Mehrmann, and Martin Schmidt. Nonlinear optimization of district heating networks. *Optimization and Engineering*, pages 1–37, 09 2020.

[17] Jarmo Söderman and Frank Pettersson. Structural and operational optimisation of distributed energy systems. *Applied Thermal Engineering*, 26(13):1400–1408, 2006. Process Integration, modelling and optimisation for energy saving and pollution reduction - PRES 2004.

[18] M. Casisi, P. Pinamonti, and M. Reini. Optimal lay-out and operation of combined heat power (chp) distributed generation systems. *Energy*, 34(12):2175–2183, 2009. ECOS 2007.

[19] C. Weber and N. Shah. Optimisation based design of a district energy system for an eco-town in the united kingdom. *Energy*, 36(2):1292–1308, 2011.

[20] Eugenia D. Mehleri, Haralambos Sarimveis, Nikolaos C. Markatos, and Lazaros G. Papageorgiou. A mathematical programming approach for optimal design of distributed energy systems at the neighbourhood level. *Energy*, 44(1):96–104, 2012. Integration and Energy System Engineering, European Symposium on Computer-Aided Process Engineering 2011.

[21] Akomeno Omu, Ruchi Choudhary, and Adam Boies. Distributed energy resource system optimisation using mixed integer linear programming. *Energy Policy*, 61:249–266, 2013.

[22] D. Buoro, M. Casisi, A. De Nardi, P. Pinamonti, and M. Reini. Multicriteria optimization of a distributed energy supply system for an industrial area. *Energy*, 58:128–137, 2013.

[23] Boran Morvaj, Ralph Evins, and Jan Carmeliet. Optimising urban energy systems: Simultaneous system sizing, operation and district heating network layout. *Energy*, 116:619–636, 2016.

[24] Thibaut Résimont. Optimization tool for the strategic outline and sizing of district heating networks using a geographic information system. https://orbi.uliege.be/handle/2268/260560, Working paper only available at orbi Uliège.

[25] SPI. Infos parc existant. http://www.hautssarts.be/fr/infos-parc-existant, Consulted on 15/05/2021.

[26] Christine Scharff (L'écho). Un micro-réseau électrique taille xxl se prépare sur le zoning des hauts sarts. https://www.lecho.be/entreprises/energie/un-micro-reseau-electrique-taille-xxl-se-prepare-sur-le-zoning-des-hauts-sarts 10121170.html, Consulted on 15/05/2021.

[27] NRB. Luminus construira la premiÈre Éolienne des hauts-sarts, chez nrb. https://www.nrb.be/fr/a-propos/actualites/luminus-construira-la-premiere-eolienne-des-hauts-sarts-chez-nrb#:~:text=NRB%20%3A%20volont%C3%A9%20de%20d%C3%A9veloppement%20durable&text=L'%C3%A9nergie%20produite%20sera%20autoconsomm%C3%A9e,ann%C3%A9e%203.097%20tonnes%20de%20CO2., Consulted on 17/05/2021.

[28] M.A. Tribe and R.L.W. Alpine. Scale economies and the "0.6 rule". *Engineering Costs and Production Economics*, 10(1):271–278, 1986.

[29] PrixPose. Prix d'une chaudière à gaz. https://www.prix-pose.com/chaudiere-gaz/, Consulted on 18/05/2021.

[30] Hevac. Industrial price list 2021.01 : Commercial and industrial heating. http://www.hevac.ie/v4/0940aa0c-5421-4a9b-840d-c9a2ae5d95bb/uploads/commercial_price_list_01_01_2014.pdf, Consulted on 18/05/2021.

[31] International Energy Agency. Iea energy technology essentials. https://iea.blob.core.windows.net/assets/1028bee0-2da1-4d68-8b0a-9e5e03e93690/essentials3.pdf, Consulted on 19/05/2021.

[32] Ingwald Obernberger, Gerold Thek, and Daniel Reiter. Economic evaluation of decentralised chp applications based on biomass combustion and biomass gasification. 01 2008.

[33] UK Government. Carbon emissions of different fuels. https://www.forestresearch.gov.uk/tools-and-resources/fthr/biomass-energy-resources/reference-biomass/facts-figures/carbon-emissions-of-different-fuels/, Consulted on 19/05/2021.

[34] Kai Wang, Seth Sanders, Swapnil Dubey, Fook Choo, and Fei Duan. Stirling cycle engines for recovering low and moderate temperature heat: A review. *Renewable and Sustainable Energy Reviews*, 62:89–108, 09 2016.

[35] F. Schlosser, M. Jesper, J. Vogelsang, T.G. Walmsley, C. Arpagaus, and J. Hesselbach. Large-scale heat pumps: Applications, performance, economic feasibility and industrial integration. *Renewable and Sustainable Energy Reviews*, 133:110219, 2020.

[36] Hui Li. Chapter 8 - thermal performance of various pavement materials. In Hui Li, editor, *Pavement Materials for Heat Island Mitigation*, pages 155–197. Butterworth-Heinemann, Boston, 2016.

[37] OCHSNER. Price list. `https://www.accubel.be/pdf/Liste-de-prix/Ochsner_liste-prix_EXPORT_2017_EN.pdf`, Consulted on 19/05/2021.

[38] Elisa Guelpa and Vittorio Verda. Thermal energy storage in district heating and cooling systems: A review. *Applied Energy*, 252:113474, 2019.

[39] Christoph F. Reinhart and Carlos Cerezo Davila. Urban building energy modeling – a review of a nascent field. *Building and Environment*, 97:196–202, 2016.

[40] Nelson Fumo. A review on the basics of building energy estimation. *Renewable and Sustainable Energy Reviews*, 31:53–60, 2014.

[41] K.B. Lindberg, S.J. Bakker, and I. Sartori. Modelling electric and heat load profiles of non-residential buildings for use in long-term aggregate load forecasts. *Utilities Policy*, 58:63–88, 2019.

[42] Bertrand Guillemot, Nelly RANGOD, and Youssef Riachi. A numerical model for determining hourly heating and dhw loads in district heating systems. 09 2014.

[43] Opal systems. Un micro-réseau électrique taille xxl se prépare sur le zoning des hauts sarts. `https://www.opal-systems.be/concept/`, Consulted on 17/05/2021.

[44] National Renewable Energy Laboratory. Land-use requirements of modern wind power plants in the united states. `https://www.nrel.gov/docs/fy09osti/45834.pdf`, Consulted on 19/05/2021.

[45] Energuide.be. What dimensions should be planned for photovoltaic panels? `https://www.energuide.be/en/questions-answers/what-dimensions-should-be-planned-for-photovoltaic-panels/1410/`, Consulted on 19/05/2021.

[46] CREG. A european comparison of electricity and natural gas prices for residential, small professional and large industrial consumers. `https://www.creg.be/sites/default/files/assets/Publications/Studies/F20200520EN.pdf`, Consulted on 25/05/2021.

[47] Dansfoss. Indirect heating systems. `https://www.danfoss.com/en/products/dhs/stations-and-domestic-hot-water/substations/indirect-heating-systems/#tab-overview`, Consulted on 21/05/2021.

[48] Stijn Anciaux. Promotion in belgium. `http://www.res-legal.eu/search-by-country/belgium/tools-list/c/belgium/s/res-e/t/promotion/sum/108/lpid/107/`, Consulted on 26/05/2021.

[49] Wallonie économie SPW. Aide à l'investissement. http://forms6.wallonie.be/formulaires/NoticeAideInvestissement.pdf, Consulted on 26/05/2021.

[50] Gurobi Optimization. Does my model have numerical issues? https://www.gurobi.com/documentation/9.1/refman/does_my_model_have_numeric.html, Consulted on 29/05/2021.

[51] Manuel Betancourt Schwarz. *Energy, economic and quality of service assessment using dynamic modelling and optimization for smart management of district heating networks*. Theses, Ecole nationale supérieure Mines-Télécom Atlantique ; Instituto superior técnico (Lisbonne), February 2021.

[52] Muhannad Delwati, Ahmed Ammar, and Philipp Geyer. Economic evaluation and simulation for the hasselt case study: Thermochemical district network technology vs. alternative technologies for heating. *Energies*, 12(7), 2019.

[53] Danish Energy Agency. Technology data - energy plants for electricity and district heating generation. https://ens.dk/sites/ens.dk/files/Statistik/technology_data_catalogue_for_el_and_dh_-_0009.pdf, Consulted on 18/05/2021.

[54] Danny Harvey. Reducing energy use in the buildings sector: Measures, costs, and examples. *Energy Efficiency*, 2, 05 2009.